CLNS 04/1904
hep-ph/0506245
June 23, 2005

Advanced Predictions for Moments of the $\bar{B} \to X_s\gamma$ Photon Spectrum

Matthias Neubert

Institute for High-Energy Phenomenology
Newman Laboratory for Elementary-Particle Physics, Cornell University
Ithaca, NY 14853, U.S.A.

Abstract

Based on a new, exact QCD factorization formula for the partial $\bar{B} \to X_s\gamma$ decay rate with a restriction on large photon energy, improved predictions are presented for the partial moments $\langle E_\gamma \rangle$ and $\langle E_\gamma^2 \rangle - \langle E_\gamma \rangle^2$ of the photon spectrum defined with a cut $E_\gamma \geq E_0$. In the region where $\Delta = m_b - 2E_0$ is large compared with $\Lambda_{\rm QCD}$, a theoretical description without recourse to shape functions can be obtained. However, for $\Delta \ll m_b$ it is important to separate short-distance contributions arising from different scales. The leading terms in the heavy-quark expansion of the moments receive contributions from the scales Δ and $\sqrt{m_b\Delta}$ only, but not from the hard scale m_b. For these terms, a complete scale separation is achieved at next-to-next-to-leading order in renormalization-group improved perturbation theory, including two-loop matching contributions and three-loop running. The results presented here can be used to extract the b-quark mass and the quantity μ_π^2 with excellent theoretical precision. A fit to experimental data reported by the Belle Collaboration yields $m_b^{\rm SF} = (4.62 \pm 0.10_{\rm exp} \pm 0.03_{\rm th})\,{\rm GeV}$ and $\mu_\pi^{2,{\rm SF}} = (0.11 \pm 0.19_{\rm exp} \pm 0.08_{\rm th})\,{\rm GeV}^2$ in the shape-function scheme at a scale $\mu_f = 1.5\,{\rm GeV}$, while $m_b^{\rm kin} = (4.54 \pm 0.11_{\rm exp} \pm 0.04_{\rm th})\,{\rm GeV}$ and $\mu_\pi^{2,{\rm kin}} = (0.49 \pm 0.18_{\rm exp} \pm 0.09_{\rm th})\,{\rm GeV}^2$ in the kinetic scheme at a scale $\mu_f = 1\,{\rm GeV}$.

1 Introduction

Experimental studies and theoretical analyses of inclusive decays of B mesons have steadily been refined over the past decade. The rates for semileptonic $\bar{B} \to X\, l^- \bar{\nu}$ decays provide access to the elements $|V_{cb}|$ and $|V_{ub}|$ of the quark mixing matrix. The rate for the radiative decay $\bar{B} \to X_s\gamma$ serves as a probe for new flavor- or CP-violating interactions. Shape variables, such as moments of inclusive spectra in different kinematic variables, can be used as a tool to probe non-perturbative QCD dynamics in a regime where it is controllable using systematic heavy-quark expansions. Global fits to moments of the charged-lepton energy spectrum and of the invariant hadronic-mass distribution in $\bar{B} \to X_c\, l^- \bar{\nu}$ decay not only give the currently most precise determination of $|V_{cb}|$, but also of the b-quark mass and of other hadronic parameters characterizing bound-state effects in the B meson, such as the quantity μ_π^2 related to the b-quark kinetic energy [1, 2].

Moments of the photon energy spectrum in $\bar{B} \to X_s\gamma$ decay are another source of information about such hadronic parameters. In particular, while in $\bar{B} \to X_c\, l^- \bar{\nu}$ decay one is primarily sensitive to the quark-mass difference $(m_b - m_c)$, a measurement of the average photon energy in $\bar{B} \to X_s\gamma$ decay comes close to a direct measurement of m_b. Existing predictions for these moments rely on a conventional heavy-quark expansion in powers of $\alpha_s(m_b)$ and $\Lambda_{\rm QCD}/m_b$. The usefulness of the photon-energy moments for the determination of m_b and μ_π^2 was first noted by Kapustin and Ligeti [3], who computed the terms of order α_s and $1/m_b^2$ in the heavy-quark expansion. These authors showed that moments of the photon spectrum are in many aspects simpler than the spectrum itself. Perturbative corrections to the moments of order $\beta_0\alpha_s^2$ were calculated (in part numerically) in [4], and $1/m_b^3$ corrections were studied in [5]. Recently, an all-order resummation of the $\beta_0^{n-1}\alpha_s^n$ terms was performed in [6]. In this paper, the authors stress the importance of shape-function effects in the region where E_0 is larger than about 1.85 GeV. As emphasized in [7], theoretical "biases" are introduced when moments measured in this region are compared with theoretical predictions obtained by ignoring these effects. The proposal of Benson et al. [6] is to correct for these biases in a *model-dependent way* by fitting a two-parameter shape-function model to the $\bar{B} \to X_s\gamma$ data, and then use the fitted spectrum to compute the differences between the true moments and the moments predicted using the conventional heavy-quark expansion (without shape functions). It is clear that in this way one obtains an accurate description of the cutoff dependence of the moments. However, the sensitivity of the moments to the parameters m_b and μ_π^2 now enters via the model ansatz used for the shape function. This introduces uncontrolled theoretical uncertainties, which in our opinion are underestimated in [6]. The conclusion of these authors that the naive heavy-quark expansion can be trusted for values $E_0 < 1.85$ GeV rests on the model-dependent assumption that shape-function tails and other low-scale effects are irrelevant in that case.

Here we follow a different strategy. It is well-known that in the endpoint region, where $m_b - 2E_\gamma \sim \Lambda_{\rm QCD}$, the $\bar{B} \to X_s\gamma$ photon spectrum obeys a QCD factorization formula of the type $d\Gamma/dE_\gamma \sim H \cdot J \otimes S$ [8, 9], where H accounts for hard gluon corrections associated with the scale m_b, the function J describes the properties of the final-state hadronic jet X_s with invariant mass of order $\sqrt{m_b\Lambda_{\rm QCD}}$, and the shape function S accounts for hadronic effects inside the B meson [10, 11]. It has been argued that such a formula (with functions H_i, J_i, S_i) holds

not only at leading power, but at every order in the $1/m_b$ expansion [12, 13, 14]. The question about the precise nature of the transition from the shape-function regime $m_b - 2E_\gamma \sim \Lambda_{\rm QCD}$ to the kinematic region where $m_b - 2E_\gamma \gg \Lambda_{\rm QCD}$ has recently been clarified in [15]. A key result is that integrals over the shape function weighted by arbitrary smooth functions can be expanded in terms of local-operator matrix elements as soon as the integration domain becomes sufficiently large [16, 17]. The shape function can be related to the discontinuity of the forward B-meson matrix element of the non-local heavy-quark effective theory (HQET) operator $\bar h_v(\omega + in\cdot D + i\epsilon)^{-1} h_v$, where v is the B-meson velocity, and n is a light-like vector satisfying $n^2 = 0$ and $v\cdot n = 1$. This matrix element has a branch cut along the real axis in the complex ω-plane, extending from $-\bar\Lambda \le \omega < \infty$, where $\bar\Lambda = (m_B - m_b)_{m_b\to\infty}$ is the familiar HQET parameter defined in the heavy-quark limit. It follows that integrals of the type

$$\int_{-\bar\Lambda}^{\Delta} d\omega\, S(\omega,\mu)\, f(\omega) \propto \oint_{|\omega|=\Delta} d\omega\, f(\omega)\, \langle \bar B(v)|\, \bar h_v \frac{1}{\omega + in\cdot D + i\epsilon}\, h_v\, |\bar B(v)\rangle \tag{1}$$

can be written as contour integrals along a circle of radius Δ in the complex ω-plane, as long as the weight function $f(\omega)$ is analytic inside this circle (which is always the case in practical applications) and $\Delta > \bar\Lambda$. In the case of the partial $\bar B \to X_s\gamma$ decay rate, phase space is such that the upper limit on the integral over ω is set by the parameter $\Delta \equiv m_b - 2E_0$, where E_0 denotes the lower cut on the photon energy. For $\Delta \sim \Lambda_{\rm QCD}$ the relation above is not of much use. However, for $\Delta \gg \Lambda_{\rm QCD}$ the right-hand side of (1) admits an expansion in terms of B-meson matrix elements of local HQET operators. This is an expansion in powers of $(\Lambda_{\rm QCD}/\Delta)^n$, i.e., not a conventional heavy-quark expansion. The corresponding Wilson coefficients have a perturbative expansion in powers of $\alpha_s(\mu)$, which is free of large logarithms provided that the renormalization scale used in the definition of the renormalized shape function is chosen such that $\mu \sim \Delta$. The scale dependence of the leading-order shape function $S(\omega,\mu)$ can be controlled precisely, because an exact analytic solution to its evolution equation exists in momentum space [15, 16, 18].

In previous work, we have applied this technology to derive a renormalization-group (RG) improved prediction for the partial $\bar B \to X_s\gamma$ decay rate as a function of the photon cut for values of E_0 outside the shape-function region (typically $E_0 < 2\,\text{GeV}$, such that $\Delta > 0.7\,\text{GeV}$) [15]. In that paper we have already presented a formula for the first moment of the photon spectrum. An important finding was that the first two terms in the $1/m_b$ expansion of the average photon energy do not receive any contributions from the hard scale m_b. Here we extend this analysis to the second moment. Most importantly, we include the complete set of two-loop matching corrections and three-loop anomalous-dimension effects so as to obtain predictions that are exact at next-to-next-to-leading order (NNLO) in RG-improved perturbation theory. We confirm that, in general, moments of the photon spectrum probe low-scale dynamics sensitive to the scales $\mu_0 \sim \Delta$ and $\mu_i \sim \sqrt{m_b\Delta}$. To a very good approximation, they are insensitive to physics at the scale m_b. As long as $\Delta \ll m_b$ ($\Delta \approx 1\,\text{GeV}$ for present experiments), it is thus not appropriate to compute the moments using a conventional heavy-quark expansion in powers of $\alpha_s(m_b)$ and $\Lambda_{\rm QCD}/m_b$. Compared with [15] we also include additional small corrections arising at higher orders in the $1/m_b$ expansion, and we comment on the effects of the photon-energy cut on the Lorentz boost between the B-meson rest frame and the $\Upsilon(4S)$ rest frame, which must be corrected for in the experimental analyses [19, 20, 21].

2 Factorization formula for the decay rate

2.1 Partial decay rate and moment relations

We begin by collecting some useful relations for moments of the partial $\bar{B} \to X_s\gamma$ decay rate, defined with a cut $E_\gamma \geq E_0$ on the photon energy measured in the B-meson rest frame. It is convenient to define a variable $p_+ = m_b - 2E_\gamma$, where for the time being m_b denotes the pole mass of the heavy b quark. The requirement $E_\gamma \geq E_0$ translates into $p_+ \leq \Delta = m_b - 2E_0$. As long as Δ is not too small, the partial rate can be calculated using an operator product expansion (OPE). From (1) it follows that the correct criterion for the validity of the OPE is $\Delta \gg \Lambda_{\rm QCD}$. We define

$$\Gamma_{\rm OPE}(\Delta) = \int_0^\Delta dp_+ \, \frac{d\Gamma_{\rm OPE}}{dp_+} \,, \tag{2}$$

taking into account that in the OPE the phase space is such that $0 \leq p_+ \leq m_b$. It follows from this expression that partial moments in the variable p_+, defined as

$$\langle p_+^n \rangle = \frac{\displaystyle\int_0^\Delta dp_+ \, p_+^n \, \frac{d\Gamma_{\rm OPE}}{dp_+}}{\displaystyle\int_0^\Delta dp_+ \, \frac{d\Gamma_{\rm OPE}}{dp_+}} \equiv \Delta^n \, M_n(\Delta) \,, \tag{3}$$

can be written in terms of integrals over the function $\Gamma_{\rm OPE}(\Delta)$, namely

$$M_n(\Delta) = 1 - \frac{n}{\Gamma_{\rm OPE}(\Delta)} \int_0^1 dy \, y^{n-1} \, \Gamma_{\rm OPE}(y\Delta) \,. \tag{4}$$

Given a theoretical formula for the partial rate $\Gamma_{\rm OPE}(\Delta)$, it is thus possible to derive arbitrary moments without going back to the differential spectrum itself. Note that for the application of this relation it is irrelevant that the variable $y\Delta$ is not always large compared with $\Lambda_{\rm QCD}$. As in (2), what matters is only the upper limit of the integration domain, because this sets the radius of the corresponding contour integral.

Moments of the photon energy spectrum can immediately be related to the functions $M_n(\Delta)$. In particular, central moments defined with respect to the cutoff, i.e. $\langle (E_\gamma - E_0)^n \rangle$, are linear combinations of the $M_n(\Delta)$. For the average photon energy and the variance $\sigma_E^2 \equiv \langle E_\gamma^2 \rangle - \langle E_\gamma \rangle^2$ of the photon spectrum, we then obtain

$$\begin{aligned} \langle E_\gamma \rangle - E_0 &= \frac{\Delta}{2} \, [1 - M_1(\Delta)] \,, \\ \sigma_E^2 &= \frac{\Delta^2}{4} \, [1 - 2M_1(\Delta) + M_2(\Delta)] - (\langle E_\gamma \rangle - E_0)^2 \,. \end{aligned} \tag{5}$$

The main goal of this work is to derive accurate theoretical expressions for these moments in a region where the cutoff E_0 is such that $\Lambda_{\rm QCD} \ll \Delta \ll m_b$. The first inequality ($\Lambda_{\rm QCD} \ll \Delta$) ensures that theoretical predictions can be obtained without recourse to non-perturbative shape (or bias) functions. The second inequality ($\Delta \ll m_b$) implies that the theory used to derive these predictions cannot be a conventional heavy-quark expansion in powers of $\alpha_s(m_b)$

and $\Lambda_{\rm QCD}/m_b$. Instead, one should disentangle the physics associated with the different short-distance scales $\Delta \ll \sqrt{m_b \Delta} \ll m_b$. For the partial rate $\Gamma_{\rm OPE}(\Delta)$, this has been achieved (at leading power in $1/m_b$) in [15].

Already at this stage it is instructive to ask what precision we might expect to achieve in the calculation of $\langle E_\gamma \rangle$ and σ_E^2. We will see below that the moments $M_n(\Delta)$ have an expansion in powers of α_s, $\Lambda_{\rm QCD}/\Delta$, and Δ/m_b. Since the leading terms in the expansion are known at two-loop order, it is reasonable to expect a precision on $M_n(\Delta)$ of about 3%. With $\Delta \approx 1\,\text{GeV}$, it follows that $\delta\langle E_\gamma \rangle \approx 0.015\,\text{GeV}$ and $\delta\sigma_E^2 \approx 0.08\,\text{GeV}^2$. At tree level, the theoretical expressions for the moments are $\langle E_\gamma \rangle = m_b/2 + \ldots$ and $\sigma_E^2 = \mu_\pi^2/12 + \ldots$, so that we may expect to extract the heavy-quark parameters with precision $\delta m_b \approx 30\,\text{MeV}$ and $\delta\mu_\pi^2 \approx 0.1\,\text{GeV}^2$. These estimates will be confirmed by the more elaborate study in Section 5. While the projected accuracy for the b-quark mass determination is exquisite, the extraction of μ_π^2 suffers to some extent from the fact that the hadronic contribution $\mu_\pi^2/12$ to the variance σ_E^2 competes with a large perturbative "background" of order $\alpha_s \Delta^2$.

2.2 A wonderful formula

At leading power in $1/m_b$ and next-to-leading order (NLO) in the expansion in powers of $\Lambda_{\rm QCD}/\Delta$, it is possible to write an expression for the partial rate $\Gamma_{\rm OPE}(\Delta)$ that is valid to all orders in perturbation theory, and in which nevertheless the dependence on the variable Δ enters in a very transparent way. Starting point is the factorization formula [15][1]

$$\begin{aligned}\Gamma(\Delta) &= \frac{G_F^2 \alpha}{32\pi^4} \, |V_{tb} V_{ts}^*|^2 \, m_b^3 \, \overline{m}_b^2(\mu_h) \, |H_\gamma(\mu_h)|^2 \, U_1(\mu_h, \mu_i) \, U_2(\mu_i, \mu_0) \, \frac{e^{-\gamma_E \eta}}{\Gamma(1+\eta)} \\ &\times \eta \int_{-\bar\Lambda}^{\Delta} dp_+ \int_{-\bar\Lambda}^{p_+} d\omega \, m_b \, J(m_b(p_+ - \omega), \mu_i) \int_{-\bar\Lambda}^{\omega} d\omega' \, \frac{S(\omega', \mu_0)}{\mu_0^\eta (\omega - \omega')^{1-\eta}} + \ldots \,, \end{aligned} \tag{6}$$

where the ellipses represent power corrections in $1/m_b$. Here m_b is the b-quark pole mass, and $\overline{m}_b(\mu)$ denotes the running mass defined in the $\overline{\rm MS}$ scheme. The function H_γ contains hard quantum fluctuations associated with the weak-interaction vertices in the effective weak Hamiltonian. The jet function J describes the physics of the hadronic final state X_s. The shape function S governs the soft physics associated with bound-state effects inside the B meson. The matching scales $\mu_h \sim m_b$, $\mu_i \sim \sqrt{m_b \Delta}$, and $\mu_0 \sim \Delta$ serve to separate the hard, hard-collinear, and soft components in the factorization theorem, and the RG functions U_1 and U_2 resum logarithmic corrections arising from evolution between these scales. The precise form of these objects, which can be found in [15], is irrelevant to our discussion. Finally, the variable

$$\eta = 2 \int_{\mu_0}^{\mu_i} \frac{d\mu}{\mu} \, \Gamma_{\rm cusp}[\alpha_s(\mu)] \tag{7}$$

is given in terms of an integral over the universal cusp anomalous dimension of Wilson loops with light-like segments [22]. The perturbative expansion of this quantity is discussed in Appendix A.1. The result (6) is formally independent of the choices of the matching scales. In

[1] The variable ω corresponds to $\hat\omega - \bar\Lambda$ in the notation of [15], and to $-\omega$ in the notation of [16].

practice, a residual scale dependence remains because one is forced to truncate the perturbative expansions of the various objects in the factorization formula.

Introducing the integral

$$j\Big(\ln\frac{Q^2}{\mu^2},\mu\Big)\equiv\int_0^{Q^2}dk^2\,J(k^2,\mu) \tag{8}$$

over the jet function, and changing the order of the integrations over p_+ and ω, the terms in the second line of (6) can be rewritten in the form

$$\mathbf{j}\Big(\ln\frac{m_b\mu_0}{\mu_i^2}+\partial_\eta,\mu_i\Big)\int_{-\bar\Lambda}^{\Delta}d\omega\,S(\omega,\mu_0)\left(\frac{\Delta-\omega}{\mu_0}\right)^\eta, \tag{9}$$

where we have defined

$$\mathbf{j}(L,\mu)\equiv\eta\int_0^1\frac{dz}{z^{1-\eta}}\,j\Big(L+\ln(1-z),\mu\Big)\,. \tag{10}$$

When L contains a derivative operator ∂_η, it is understood that this operator acts only to the right.

The remaining shape-function integral is of the type shown in (1), and for $\Delta\gg\Lambda_{\rm QCD}$ it can be expanded in matrix elements of local HQET operators. To this end, we replace the true shape function by the corresponding function obtained in the parton model with on-shell external quark states, which has support for $\omega\geq-n\cdot k$ instead of $\omega\geq-\bar\Lambda$, where $k=p_b-m_bv$ with $v\cdot k=0$ is the residual momentum of the on-shell heavy quark. We then evaluate the integral, expand the result in powers of $n\cdot k$, and match the answer onto HQET matrix elements [16]. It is convenient to use an integration by parts and introduce the integral

$$s\Big(\ln\frac{\Omega_k}{\mu},\mu\Big)\equiv\int_{-n\cdot k}^{\Omega}d\omega\,S_{\rm parton}(\omega,\mu)\,, \tag{11}$$

which is analogous to the function j in (8). Reparameterization invariance [23, 24] ensures that the result only depends on the sum $\Omega_k=\Omega+n\cdot k$. Introducing a related function

$$\mathbf{s}(L,\mu)\equiv\eta\int_0^1\frac{dz}{z^{1-\eta}}\,s\Big(L+\ln(1-z),\mu\Big) \tag{12}$$

in analogy with (10), we find that

$$\begin{aligned}\int_{-\bar\Lambda}^{\Delta}d\omega\,S_{\rm parton}(\omega,\mu_0)\left(\frac{\Delta-\omega}{\mu_0}\right)^\eta&=\frac{\eta}{\mu_0}\int_{-n\cdot k}^{\Delta}d\omega\left(\frac{\Delta-\omega}{\mu_0}\right)^{\eta-1}s\Big(\ln\frac{\omega+n\cdot k}{\mu_0},\mu_0\Big)\\&=\mathbf{s}\left(\partial_\eta,\mu_0\right)\left(\frac{\Delta+n\cdot k}{\mu_0}\right)^\eta.\end{aligned} \tag{13}$$

We now expand this result to second order in $n\cdot k$ and replace $n\cdot k\to0$, $(n\cdot k)^2\to\mu_\pi^2/3$, which accomplishes the matching onto local HQET matrix elements to first non-trivial order. This yields to the following result for the terms in the second line of the factorization formula (6):

$$\mathbf{j}\Big(\ln\frac{m_b\mu_0}{\mu_i^2}+\partial_\eta,\mu_i\Big)\,\mathbf{s}\left(\partial_\eta,\mu_0\right)\left(\frac{\Delta}{\mu_0}\right)^\eta\left[1-\frac{\eta(1-\eta)}{6}\,\frac{\mu_\pi^2}{\Delta^2}+\ldots\right]. \tag{14}$$

It remains to derive the explicit form of the functions $\mathbf{j}$ and $\mathbf{s}$. This can be accomplished by noting that at any order in perturbation theory the objects $j(L,\mu)$ and $s(L,\mu)$ are polynomials in L (see Section 2.3 below), so that it suffices to compute the integrals

$$\begin{aligned}
&\eta \int_0^1 \frac{dz}{z^{1-\eta}} \left(L + \partial_\eta + \ln(1-z)\right)^n = \partial_\epsilon^n \int_0^1 dz\, \eta\, z^{\eta-1} \left((1-z)\, e^{L+\partial_\eta}\right)^\epsilon \Big|_{\epsilon=0} \\
&= \partial_\epsilon^n \frac{\Gamma(1+\eta)\,\Gamma(1+\epsilon)}{\Gamma(1+\eta+\epsilon)}\, e^{\epsilon(L+\partial_\eta)}\Big|_{\epsilon=0} \equiv \frac{\Gamma(1+\eta)}{e^{-\gamma_E\eta}}\, I_n(L+\partial_\eta)\, \frac{e^{-\gamma_E\eta}}{\Gamma(1+\eta)}\,, \qquad (15)
\end{aligned}$$

where

$$I_n(x) = \partial_\epsilon^n \left[e^{\epsilon(x+\gamma_E)}\,\Gamma(1+\epsilon)\right]_{\epsilon=0} = \partial_\epsilon^n \exp\left[\epsilon x + \sum_{k=2}^\infty \frac{(-1)^k}{k}\,\epsilon^k \zeta_k\right]_{\epsilon=0} \qquad (16)$$

are polynomials of degree n. For our purposes we need the first four of them, which are

$$\begin{aligned}
I_1(x) &= x\,, & I_3(x) &= x^3 + \frac{\pi^2}{2}\,x - 2\zeta_3\,, \\
I_2(x) &= x^2 + \frac{\pi^2}{6}\,, & I_4(x) &= x^4 + \pi^2 x - 8\zeta_3\,x + \frac{3\pi^4}{20}\,. \qquad (17)
\end{aligned}$$

We now define functions $\widetilde{s}$ and $\widetilde{j}$ by the following replacement rules:

$$\widetilde{j}(L,\mu) \equiv j(L,\mu)\Big|_{L^n\to I_n(L)}\,, \qquad \widetilde{s}(L,\mu) \equiv s(L,\mu)\Big|_{L^n\to I_n(L)}\,. \qquad (18)$$

It follows that

$$\mathbf{j}(L+\partial_\eta,\mu) = \frac{\Gamma(1+\eta)}{e^{-\gamma_E\eta}}\,\widetilde{j}(L+\partial_\eta,\mu)\,\frac{e^{-\gamma_E\eta}}{\Gamma(1+\eta)}\,, \qquad (19)$$

and similarly for the soft function. The exact result for the leading-power contribution to the partial decay rate in the OPE can now be written in the remarkable form

$$\begin{aligned}
\Gamma_{\rm OPE}(\Delta) &= \frac{G_F^2\alpha}{32\pi^4}\,|V_{tb}V_{ts}^*|^2\, m_b^3\, \overline{m}_b^2(\mu_h)\,|H_\gamma(\mu_h)|^2\, U_1(\mu_h,\mu_i)\, U_2(\mu_i,\mu_0) \qquad (20) \\
&\times \left\{\widetilde{j}\Big(\ln\frac{m_b\mu_0}{\mu_i^2} + \partial_\eta, \mu_i\Big)\,\widetilde{s}\,(\partial_\eta,\mu_0)\,\frac{e^{-\gamma_E\eta}}{\Gamma(1+\eta)}\left(\frac{\Delta}{\mu_0}\right)^\eta \left[1 - \frac{\eta(1-\eta)}{6}\,\frac{\mu_\pi^2}{\Delta^2} + \ldots\right] + \mathcal{O}\left(\frac{\Delta}{m_b}\right)\right\}.
\end{aligned}$$

This result implies that for $m_b - 2E_\gamma \gg \Lambda_{\rm QCD}$ the photon spectrum exhibits a radiation tail, $d\Gamma/dE_\gamma \propto 1/(m_b-2E_\gamma)^{1-\eta}$ modulo small logarithmic corrections, which falls off slowly with energy. The presence of this tail and its phenomenological implications have been discussed in [15]. Note that even at leading power in $1/m_b$ there exist non-perturbative corrections of the form $(\Lambda_{\rm QCD}/\Delta)^n$ with $n \geq 2$. We have included the leading such term, which is proportional to the kinetic-energy parameter μ_π^2. For $\Delta \sim 1\,\text{GeV}$ the numerical impact of these power corrections is rather small, so it seems safe to truncate the series at this point.

It is worth emphasizing that expression (20) is exact to all orders in perturbation theory, and it is valid for any values of the matching scales μ_h, μ_i, and μ_0. In the limit where all three matching scale are set equal to a common scale μ, the result smoothly reduces to conventional

fixed-order perturbation theory. While the resummed, factorized expression is superior to a fixed-order result whenever there are widely separated scales in the problem (i.e., for $\Delta \ll m_b$), it remains valid in the limit where the different scales become of the same order ($\Delta \sim m_b$).[2] In other words, there is never a region where fixed-order perturbation theory would be more appropriate to use than the above factorization formula.

2.3 Evolution equations and two-loop results

The functions $j(L,\mu)$ and $s(L,\mu)$ obey integro-differential RG equations, which can be derived starting from the evolution equations for the jet and shape functions discussed in [15, 16]. We find

$$\begin{aligned}
\frac{d}{d\ln\mu}\, j(L,\mu) &= -2\Big[\Gamma_{\rm cusp}(\alpha_s)\, L + \gamma^J(\alpha_s)\Big]\, j(L,\mu) \\
&\quad - 2\Gamma_{\rm cusp}(\alpha_s) \int_0^1 \frac{dz}{z} \Big[j(L+\ln(1-z),\mu) - j(L,\mu)\Big]\,, \\
\frac{d}{d\ln\mu}\, s(L,\mu) &= 2\Big[\Gamma_{\rm cusp}(\alpha_s)\, L - \gamma(\alpha_s)\Big]\, s(L,\mu) \\
&\quad + 2\Gamma_{\rm cusp}(\alpha_s) \int_0^1 \frac{dz}{z} \Big[s(L+\ln(1-z),\mu) - s(L,\mu)\Big]\,,
\end{aligned} \tag{21}$$

where $\alpha_s \equiv \alpha_s(\mu)$. We encounter again the cusp anomalous dimension $\Gamma_{\rm cusp}$, and in addition anomalous dimensions γ and γ^J governing the single-logarithmic evolution of the shape and jet functions, respectively. (Recall that for j we have $L = \ln(Q^2/\mu^2)$, while for s we have instead $L = \ln(\Omega_k/\mu)$.) These equations can be solved order by order in perturbation theory with a double-logarithmic expansion of the form

$$\begin{aligned}
j(L,\mu) &= 1 + \sum_{n=1}^{\infty} \left(\frac{\alpha_s(\mu)}{4\pi}\right)^n \Big(b_0^{(n)} + b_1^{(n)} L + \ldots + b_{2n-1}^{(n)} L^{2n-1} + b_{2n}^{(n)} L^{2n}\Big)\,, \\
s(L,\mu) &= 1 + \sum_{n=1}^{\infty} \left(\frac{\alpha_s(\mu)}{4\pi}\right)^n \Big(c_0^{(n)} + c_1^{(n)} L + \ldots + c_{2n-1}^{(n)} L^{2n-1} + c_{2n}^{(n)} L^{2n}\Big)\,.
\end{aligned} \tag{22}$$

The evolution equations (21) allow us to express all coefficients of logarithms in terms of the perturbative expansion coefficients of the anomalous dimensions and β function. At two-loop order, we obtain

$$\begin{aligned}
j(L,\mu) &= 1 + \frac{\alpha_s(\mu)}{4\pi}\left[b_0^{(1)} + \gamma_0^J L + \frac{1}{2}\,\Gamma_0 L^2\right] \\
&\quad + \left(\frac{\alpha_s(\mu)}{4\pi}\right)^2 \left[b_0^{(2)} + \left(b_0^{(1)}(\gamma_0^J - \beta_0) + \gamma_1^J - \frac{\pi^2}{6}\,\Gamma_0\gamma_0^J + \zeta_3\Gamma_0^2\right) L \right. \\
&\quad \left. + \frac{1}{2}\left(\gamma_0^J(\gamma_0^J - \beta_0) + b_0^{(1)}\,\Gamma_0 + \Gamma_1 - \frac{\pi^2}{6}\,\Gamma_0^2\right) L^2 - \left(\frac{1}{6}\,\beta_0 - \frac{1}{2}\gamma_0^J\right)\Gamma_0 L^3 + \frac{1}{8}\,\Gamma_0^2 L^4\right],
\end{aligned}$$

[2] In this case, of course, power corrections of order Δ/m_b would become important.

$$
\begin{aligned}
s(L,\mu) &= 1 + \frac{\alpha_s(\mu)}{4\pi}\left[c_0^{(1)} + 2\gamma_0 L - \Gamma_0 L^2\right] \\
&\quad + \left(\frac{\alpha_s(\mu)}{4\pi}\right)^2 \left[c_0^{(2)} + \left(2c_0^{(1)}(\gamma_0-\beta_0) + 2\gamma_1 + \frac{2\pi^2}{3}\,\Gamma_0\gamma_0 + 4\zeta_3\Gamma_0^2\right) L \right. \\
&\quad \left. + \left(2\gamma_0(\gamma_0-\beta_0) - c_0^{(1)}\Gamma_0 - \Gamma_1 - \frac{\pi^2}{3}\,\Gamma_0^2\right) L^2 + \left(\frac{2}{3}\,\beta_0 - 2\gamma_0\right)\Gamma_0 L^3 + \frac{1}{2}\,\Gamma_0^2 L^4\right],
\end{aligned}
\tag{23}
$$

where [16, 17]

$$
b_0^{(1)} = (7-\pi^2)\,C_F\,, \qquad c_0^{(1)} = -\frac{\pi^2}{6}\,C_F\,, \tag{24}
$$

and the coefficients $b_0^{(2)}$ and $c_0^{(2)}$ are unknown. The relevant expansion coefficients of the anomalous dimensions and β functions are listed in Appendices A.1 and A.2.

3 Ingredients of the moment calculation

3.1 Results at leading power in $1/m_b$

While the result (20) is of considerable complexity when expanded beyond the leading order in RG-improved perturbation theory, it is well suited for computing the moments $M_n(\Delta)$ using relation (4). The reason is that, *before* the derivatives with respect to η are carried out, the dependence on Δ is of power type. According to (4) the moments $M_n(\Delta)$ are obtained from ratios of expressions linear in the decay rate, and hence any Δ-independent factors cancel out. It follows that the entire first line in (20), and in particular all reference to the hard scale μ_h, cancels in the formulae for the moments. (A very weak dependence on the hard scale enters through the $1/m_b$ corrections, see below.) Also, after the integral over y in (4) has been carried out, the product $[e^{-\gamma_E\eta}/\Gamma(1+\eta)]\,(\Delta/\mu_0)^\eta$ can be pulled through the differential operators $\widetilde{s}$ and $\widetilde{j}$ using that

$$
\partial_\eta\,\frac{e^{-\gamma_E\eta}}{\Gamma(1+\eta)}\left(\frac{\Delta}{\mu_0}\right)^\eta f(\eta) = \frac{e^{-\gamma_E\eta}}{\Gamma(1+\eta)}\left(\frac{\Delta}{\mu_0}\right)^\eta \left(\ln\frac{\Delta}{\mu_0} - h(\eta) + \partial_\eta\right) f(\eta)\,, \tag{25}
$$

where $h(\eta) = \psi(1+\eta) + \gamma_E$. It is then immediate to obtain the following, exact form for the moments at leading power in $1/m_b$, indicated with a superscript "(0)":

$$
M_n^{(0)}(\Delta) = 1 - \frac{\mathcal{D}(\nabla_\eta)\left[\dfrac{n}{n+\eta} - \dfrac{n}{n+\eta-2}\,\dfrac{\eta(1-\eta)}{6}\,\dfrac{\mu_\pi^2}{\Delta^2} + \ldots\right]}{\mathcal{D}(\nabla_\eta)\left[1 - \dfrac{\eta(1-\eta)}{6}\,\dfrac{\mu_\pi^2}{\Delta^2} + \ldots\right]}\,. \tag{26}
$$

The object

$$
\mathcal{D}(\nabla_\eta) = \widetilde{j}\Big(\ln\frac{m_b\Delta}{\mu_i^2} + \nabla_\eta\Big)\,\widetilde{s}(\ln\frac{\Delta}{\mu_0} + \nabla_\eta)\,; \qquad \nabla_\eta = \frac{d}{d\eta} - h(\eta) \tag{27}
$$

is a differential operator defined in terms of the functions $\widetilde{j}$ and $\widetilde{s}$, which are determined in terms of the matching corrections at the hard-collinear and soft scales, μ_i and μ_0, respectively. A careful analysis of the equations that led to (20) shows that the result for the μ_π^2 term in the numerator of (26) is correct for any positive integer n, even though the integral over y in (4) appears to diverge for $n < 2$. At two-loop order $\mathcal{D}(\nabla_\eta)$ is a fourth-order polynomial in ∇_η. It is understood that the derivatives with respect to η in an expression of the form $\mathcal{D}(\nabla_\eta)\, f(\eta)$ act on both $f(\eta)$ and the function $h(\eta)$ in the definition of ∇_η, e.g. $\nabla_\eta^2\, f(\eta) = f''(\eta) - 2h(\eta)\, f'(\eta) - h'(\eta)\, f(\eta) + h^2(\eta)\, f(\eta)$. Note the important fact that the unknown two-loop coefficients $b_0^{(2)}$ and $c_0^{(2)}$ in (23) cancel in the ratio (26). This means that we have all the ingredients in place to obtain predictions for the moments M_n that are valid at NNLO in RG-improved perturbation theory. At this order, exact two-loop matching conditions at the scales μ_i and μ_0 are combined with three-loop running effects incorporated in the calculation of the parameter η, which resums logarithms of the ratio $(\mu_i/\mu_0)^2 \sim m_b/\Delta$.

Eqs. (20) and (26) are the main results of this work. It is straightforward to work out the leading-power contributions to the moments $M_1(\Delta)$ and $M_2(\Delta)$ by carrying out the derivatives with respect to η in (26) and expanding the resulting expression consistently in powers of $\alpha_s(\mu_i)$, $\alpha_s(\mu_0)$ and to first order in μ_π^2/Δ^2. At NLO in RG-improved perturbation theory, we find

$$\begin{aligned}
M_1^{(0)}(\Delta) &= \frac{1}{(1+\eta)^2}\left\{\left(1-\frac{\mu_\pi^2}{3\Delta^2}\right)\left[\eta(1+\eta)+\frac{C_F\alpha_s(\mu_i)}{\pi}\left(\ln\frac{m_b\Delta}{\mu_i^2}-h(\eta)-\frac{3}{4}-\frac{1}{1+\eta}\right)\right.\right.\\
&\qquad\left.+\frac{C_F\alpha_s(\mu_0)}{\pi}\left(-2\ln\frac{\Delta}{\mu_0}+2h(\eta)-1+\frac{2}{1+\eta}\right)\right]\\
&\qquad\left.+\frac{\mu_\pi^2}{3\Delta^2}\,(1-2\eta)\left[\frac{C_F\alpha_s(\mu_0)}{\pi}-\frac{C_F\alpha_s(\mu_i)}{2\pi}\right]\right\},\\
M_2^{(0)}(\Delta) &= \frac{2}{(2+\eta)^2}\left\{\left(1-\frac{\mu_\pi^2}{\Delta^2}\right)\left[\frac{\eta(2+\eta)}{2}+\frac{C_F\alpha_s(\mu_i)}{\pi}\left(\ln\frac{m_b\Delta}{\mu_i^2}-h(\eta)-\frac{3}{4}-\frac{1}{2+\eta}\right)\right.\right.\\
&\qquad\left.+\frac{C_F\alpha_s(\mu_0)}{\pi}\left(-2\ln\frac{\Delta}{\mu_0}+2h(\eta)-1+\frac{2}{2+\eta}\right)\right]\\
&\qquad\left.+\frac{\mu_\pi^2}{3\Delta^2}\,(1-2\eta)\left[\frac{C_F\alpha_s(\mu_0)}{\pi}-\frac{C_F\alpha_s(\mu_i)}{2\pi}\right]\right\}+\frac{\mu_\pi^2}{3\Delta^2}\,. \qquad (28)
\end{aligned}$$

The corresponding expressions valid at NNLO are far more complicated. We do not list them explicitly, as it is easiest to generate them directly from (26). In the resulting formulae one should expand the quantity η consistently to the required order in RG-improved perturbation theory, using the results compiled in Appendix A.1. (Using instead the NNLO expression for η everywhere makes a negligible difference in our numerical results.) Also, before applying these results to the analysis of experimental data, the pole-scheme parameters m_b and μ_π^2 should be eliminated in favor of corresponding parameters defined in a physical renormalization scheme.

The scale separation achieved using RG techniques, which allows us to disentangle the physics at the hard, hard-collinear, and soft scales (m_b, $\sqrt{m_b\Delta}$, and Δ), is one of the most

important ingredients of our approach. This, combined with the fact that for the first time we include the complete two-loop perturbative corrections, distinguishes our calculation from all previous analyses of the $\bar{B} \to X_s\gamma$ moments. The physical insight that the shape variables probe low-scale dynamics, while at leading power in $1/m_b$ they are insensitive to physics at the hard scale m_b, makes it apparent that a precise control over low-scale perturbative corrections is crucial to obtain reliable predictions for the moments.

In order to compare our RG-improved results with those of the conventional heavy-quark approach, it is useful to expand expression (26) to two-loop order in fixed-order perturbation theory. We obtain

$$\begin{aligned}
M_1^{(0)}(\Delta) &= \left(1-\frac{\mu_\pi^2}{3\Delta^2}\right)\frac{C_F\alpha_s(\mu)}{\pi}\left[-\ln\frac{\Delta}{m_b}-\frac{3}{4}+\frac{\alpha_s(\mu)}{\pi}\,k_1(\Delta)\right] \\
&\quad+\frac{\mu_\pi^2}{3\Delta^2}\,\frac{C_F\alpha_s(\mu)}{\pi}\left[\frac{1}{2}+\frac{\alpha_s(\mu)}{\pi}\,k_2(\Delta)\right], \\
M_2^{(0)}(\Delta) &= \left(1-\frac{\mu_\pi^2}{\Delta^2}\right)\frac{C_F\alpha_s(\mu)}{\pi}\left[-\frac{1}{2}\ln\frac{\Delta}{m_b}-\frac{5}{8}+\frac{\alpha_s(\mu)}{\pi}\,k_3(\Delta)\right] \\
&\quad+\frac{\mu_\pi^2}{3\Delta^2}\left[1+\frac{C_F\alpha_s(\mu)}{4\pi}+C_F\left(\frac{\alpha_s(\mu)}{\pi}\right)^2 k_4(\Delta)\right],
\end{aligned} \tag{29}$$

where the two-loop coefficients are given by

$$\begin{aligned}
k_1(\Delta) &= \left(\frac{3\beta_0}{8}-C_F\right)\ln^2\frac{\Delta}{m_b}+\left[\left(\frac{1}{2}\ln\frac{m_b}{\mu}-\frac{23}{48}\right)\beta_0-\left(\frac{1}{2}+\frac{\pi^2}{6}\right)C_F-\left(\frac{1}{3}-\frac{\pi^2}{12}\right)C_A\right]\ln\frac{\Delta}{m_b} \\
&\quad+\left(\frac{3}{8}\ln\frac{m_b}{\mu}-\frac{13}{32}+\frac{\pi^2}{24}\right)\beta_0-\left(\frac{29}{32}+\frac{\zeta_3}{2}\right)C_F+\left(\frac{7}{16}+\frac{\zeta_3}{4}\right)C_A\,, \\
k_2(\Delta) &= \left(2C_F-\frac{3\beta_0}{8}\right)\ln\frac{\Delta}{m_b}-\left(\frac{1}{4}\ln\frac{m_b}{\mu}-\frac{59}{96}\right)\beta_0+\left(1+\frac{\pi^2}{12}\right)C_F+\left(\frac{1}{6}-\frac{\pi^2}{24}\right)C_A\,, \\
k_3(\Delta) &= \left(\frac{3\beta_0}{16}-\frac{C_F}{4}\right)\ln^2\frac{\Delta}{m_b}+\left[\left(\frac{1}{4}\ln\frac{m_b}{\mu}-\frac{5}{96}\right)\beta_0-\left(\frac{1}{2}+\frac{\pi^2}{12}\right)C_F-\left(\frac{1}{6}-\frac{\pi^2}{24}\right)C_A\right]\ln\frac{\Delta}{m_b} \\
&\quad+\left(\frac{5}{16}\ln\frac{m_b}{\mu}-\frac{5}{12}+\frac{\pi^2}{48}\right)\beta_0-\left(\frac{11}{32}+\frac{\pi^2}{24}+\frac{\zeta_3}{4}\right)C_F+\left(\frac{13}{96}+\frac{\pi^2}{48}+\frac{\zeta_3}{8}\right)C_A\,, \\
k_4(\Delta) &= \left(\frac{3C_F}{4}-\frac{3\beta_0}{16}\right)\ln\frac{\Delta}{m_b}-\left(\frac{1}{8}\ln\frac{m_b}{\mu}-\frac{41}{192}\right)\beta_0+\left(\frac{7}{8}+\frac{\pi^2}{24}\right)C_F+\left(\frac{1}{12}-\frac{\pi^2}{48}\right)C_A\,.
\end{aligned} \tag{30}$$

The terms of order α_s and $\beta_0\alpha_s^2$ in these expressions agree with those obtained in [4]. However, above we include the complete set of two-loop corrections. Very recently, the dominant part of the $\bar{B} \to X_s\gamma$ photon spectrum has been calculated at $O(\alpha_s^2)$ [25]. Using the results of that paper to calculate the moments $M_n^{(0)}(\Delta)$, we find complete agreement with our expressions for the functions k_1 and k_3. We stress that both of these coefficients contain a contribution proportional to the combination $(2\gamma_1+\gamma_1^J)$ of the two-loop anomalous dimensions of the shape

and jet functions. The agreement with [25] therefore serves as a test of the expressions for the anomalous dimensions collected in Appendix A.2.

Our expressions for the μ_π^2/Δ^2 power corrections to the moments are new, except for the tree-level contribution to $M_2^{(0)}(\Delta)$, which agrees with [3]. Prior to this work, power corrections proportional to the HQET parameter μ_π^2 have never been computed beyond the tree approximation. Here, we have calculated the Wilson coefficients of these terms at two-loop order.

3.2 Power corrections in $1/m_b$

The power-suppressed corrections to the moments $M_n(\Delta)$ can be separated into two classes: "kinematic" corrections of order $(\Delta/m_b)^k$, and "hadronic" corrections involving non-perturbative heavy-quark parameters. The kinematic corrections are known to $O(\alpha_s)$ in fixed-order perturbation theory, without scale separation and RG improvement. The Wilson coefficients of the operators contributing to the hadronic power corrections are known at tree level up to and including terms of order $\Lambda_{\rm QCD}^3$ in the heavy-quark expansion. The corresponding contributions to the moments are so small that radiative corrections to these Wilson coefficients are unlikely to have any significant impact. The two types of corrections are linked to each other and should be combined consistently order by order in the $1/m_b$ expansion. When we will introduce heavy-quark parameters defined in physical renormalization schemes in Section 3.3, a reshuffling of terms between the kinematic and hadronic corrections will take place.

We begin with a review of the kinematic power corrections. In fixed-order perturbation theory, they are due to contributions from real-gluon emission graphs ($b\to s\gamma g$ at the parton level) that are phase-space suppressed in the endpoint region. The corresponding contributions to the partial decay rate can be included by adding the term

$$\frac{C_F\alpha_s(\mu)}{4\pi}\sum_{i\le j}\mathrm{Re}\,\frac{C_i^*(\mu_h)\,C_j(\mu_h)}{|C_7(\mu_h)|^2}\,3f_{ij}(\delta) \tag{31}$$

inside the curly brackets in the second line of (20). Here $\delta=\Delta/m_b$, and i,j take the values $1,7,8$, corresponding to different operators in the effective weak Hamiltonian for $\bar B\to X_s\gamma$ decay. The coefficients $C_7\equiv C_{7\gamma}^{\rm eff}$ and $C_8\equiv C_{8g}^{\rm eff}$ are the "effective" Wilson coefficients of the electro-magnetic and chromo-magnetic dipole operators, while C_1 is the coefficient of the current–current operator $(\bar sc)_{V-A}(\bar cb)_{V-A}$. Operators other than these three can be safely neglected. The coefficients C_i are evaluated at a hard scale $\mu_h\sim m_b$. This will be implicitly understood in the equations below. On the other hand, given that the emitted gluon is part of the final-state hadronic jet X_s, an appropriate choice for the scale μ in the coupling constant in (31) is more likely to be one of the low scales μ_i or μ_0. In our numerical analysis in Section 5 we set $\mu=\mu_i$ but vary both scales independently to be conservative.

In the Standard Model the Wilson coefficients are real, and we will thus drop the "Re" symbol below. Explicit expressions for the kinematic functions $f_{ij}(\delta)$ can be found in [7]. To first order in α_s, the moments $M_n(\Delta)$ receive an additive contribution from the kinematic power corrections given by

$$M_n(\Delta)\Big|_{\rm kin}=\frac{C_F\alpha_s(\mu)}{\pi}\sum_{i\le j}\frac{C_iC_j}{C_7^2}\,\frac{3}{4}\left[f_{ij}(\delta)-n\int_0^1 dy\,y^{n-1}f_{ij}(y\delta)\right], \tag{32}$$

where $C_i \equiv C_i(\mu_h)$. For the case $n = 1$ the expressions in brackets were called $-d_{ij}(\delta)/\delta$ in [7], where explicit forms for these functions can be found. For our purposes it will be sufficient to expand the results in powers of δ. The dominant contribution comes from the case where $i = j = 7$, corresponding to weak decay mediated by the electro-magnetic dipole operator in the effective weak Hamiltonian. For this term, we also include the two-loop perturbative corrections, which can be extracted from the formulae given in [25]. Two-loop corrections involving other Wilson coefficients are presently unknown, but their effects on the moments are bound to be negligible.

Non-perturbative hadronic corrections of leading and subleading order were calculated in [3, 5], respectively. These authors find

$$\begin{aligned} M_1(\Delta)\Big|_{\rm hadr} &= \frac{\lambda_1 + 3\lambda_2}{2m_b\Delta} + \frac{5\rho_1 - 21\rho_2}{6m_b^2\Delta} + \frac{\mathcal{T}_1 + 3\mathcal{T}_2 + \mathcal{T}_3 + 3\mathcal{T}_4}{2m_b^2\Delta} + \dots , \\ M_2(\Delta)\Big|_{\rm hadr} &= -\frac{\lambda_1}{3\Delta^2} - \frac{2\rho_1 - 3\rho_2}{3m_b\Delta^2} - \frac{\mathcal{T}_1 + 3\mathcal{T}_2}{3m_b\Delta^2} + \dots , \end{aligned} \tag{33}$$

where λ_i [26], ρ_i [27], and $\mathcal{T}_i$ [28] are hadronic matrix elements defined in HQET. Note that the leading term in the expression for the second moment is not power suppressed in $1/m_b$. It is already included in the leading-order prediction for that moment in (28). In theoretical expressions for inclusive decay distributions, the parameters $\mathcal{T}_i$ always appear in the same combinations with λ_1 and λ_2, and it is thus convenient to absorb them into a redefinition of these parameters, such that

$$\hat\lambda_1 = \lambda_1 + \frac{\mathcal{T}_1 + 3\mathcal{T}_2}{m_b} , \qquad \hat\lambda_2 = \lambda_2 + \frac{\mathcal{T}_3 + 3\mathcal{T}_4}{3m_b} . \tag{34}$$

Then the only place where the $\mathcal{T}_i$ parameters appear is in spectroscopy. For instance, at tree level the spin splitting between the ground-state heavy mesons is given by [28]

$$m_{B^*} - m_B = \frac{2\hat\lambda_2}{m_b} - \frac{\rho_2 - \mathcal{T}_2 + \frac{2}{3}\mathcal{T}_3 + \mathcal{T}_4}{m_b^2} + \dots , \tag{35}$$

which in essence means that there is an uncertainty of relative order $\Lambda_{\rm QCD}/m_b$ in the determination of the parameter $\hat\lambda_2$. For the purposes of the present work we adopt the conventions introduced in [29], which are such that

$$\mu_\pi^2 = -\hat\lambda_1 , \qquad \mu_G^2 = 3\hat\lambda_2 , \qquad \rho_D^3 = \rho_1 , \qquad \rho_{LS}^3 = 3\rho_2 . \tag{36}$$

For the time being all definitions still refer to the pole scheme.

Combining the contributions from kinematic and hadronic power corrections, we find that the first-order corrections to the moments are

$$\begin{aligned} M_1^{(1)}(\Delta) = \frac{\Delta}{m_b}\Bigg\{ &\frac{\mu_G^2 - \mu_\pi^2}{2\Delta^2} + \frac{C_F\alpha_s(\mu)}{\pi}\Bigg[1 - \frac{1}{2}\ln\frac{\Delta}{m_b} + \frac{\alpha_s(\mu)}{\pi}\,l_1(\Delta) + \frac{2}{9}\,\frac{C_1^2}{C_7^2}\,g_2(z) \\ &+ \frac{5}{12}\,\frac{C_8}{C_7} - \frac{1}{3}\left(\frac{C_1}{C_7} - \frac{C_1C_8}{3C_7^2}\right)g_1(z) + \frac{1}{18}\,\frac{C_8^2}{C_7^2}\left(\ln\frac{m_b}{m_s} - 1 + \frac{1}{2}\ln\frac{\Delta}{m_b}\right)\Bigg]\Bigg\} , \end{aligned}$$

$$M_2^{(1)}(\Delta) = \frac{\Delta}{m_b}\left\{ -\frac{2\rho_D^3-\rho_{LS}^3}{3\Delta^3} + \frac{C_F\alpha_s(\mu)}{\pi}\left[\frac{11}{18} - \frac{1}{3}\ln\frac{\Delta}{m_b} + \frac{\alpha_s(\mu)}{\pi}\,l_2(\Delta) + \frac{4}{27}\,\frac{C_1^2}{C_7^2}\,g_2(z)\right.\right.$$
$$\left.\left. + \frac{5}{18}\,\frac{C_8}{C_7} - \frac{2}{9}\left(\frac{C_1}{C_7} - \frac{C_1C_8}{3C_7^2}\right)g_1(z) + \frac{1}{27}\,\frac{C_8^2}{C_7^2}\left(\ln\frac{m_b}{m_s} - \frac{11}{12} + \frac{1}{2}\ln\frac{\Delta}{m_b}\right)\right]\right\}, \quad (37)$$

where we have ordered the various contributions in magnitude. The combined result for the second-order power correction to the first moment reads

$$M_1^{(2)}(\Delta) = \left(\frac{\Delta}{m_b}\right)^2\left\{\frac{5\rho_D^3-7\rho_{LS}^3}{6\Delta^3} + \frac{C_F\alpha_s(\mu)}{\pi}\left[\frac{7}{36} + \frac{1}{6}\ln\frac{\Delta}{m_b} + \frac{\alpha_s(\mu)}{\pi}\,l_3(\Delta)\right.\right.$$
$$+ \frac{C_8}{C_7}\left(-\frac{5}{27} + \frac{2}{9}\ln\frac{\Delta}{m_b}\right) + \frac{2}{9}\left(\frac{C_1}{C_7} - \frac{C_1C_8}{3C_7^2}\right)g_3(z)$$
$$\left.\left. + \frac{1}{27}\,\frac{C_8^2}{C_7^2}\left(\ln\frac{m_b}{m_s} - \frac{11}{12} + \frac{1}{2}\ln\frac{\Delta}{m_b}\right)\right]\right\}. \quad (38)$$

In these expressions,

$$g_1(z) = \int_0^1 dx\,x\,\mathrm{Re}\left[\frac{z}{x}\,G\Big(\frac{x}{z}\Big) + \frac{1}{2}\right],$$
$$g_2(z) = \int_0^1 dx\,(1-x)\left|\frac{z}{x}\,G\Big(\frac{x}{z}\Big) + \frac{1}{2}\right|^2,$$
$$g_3(z) = \mathrm{Re}\left[z\,G\Big(\frac{1}{z}\Big) + \frac{1}{2}\right], \quad (39)$$

with

$$G(t) = \begin{cases} -2\arctan^2\sqrt{t/(4-t)} & ;\ t<4\,, \\ 2\left(\ln\Big[(\sqrt{t}+\sqrt{t-4})/2\Big] - \dfrac{i\pi}{2}\right)^2 & ;\ t\geq 4\,, \end{cases} \quad (40)$$

are functions of the mass ratio $z=(m_c/m_b)^2$, which arise from charm-penguin loop diagrams. The logarithms of the quark-mass ratio m_b/m_s arise due to a collinear singularity in the process $b\to sg$ mediated by the operator Q_{8g}, followed by photon emission off the strange quark. This contribution is so small that a more careful treatment of these logarithms is not necessary. The $O(\alpha_s^2)$ corrections to the electro-magnetic dipole contributions in (37) and (38) are encoded in the coefficients

$$l_1(\Delta) = \left(\frac{3\beta_0}{16} - C_F\right)\ln^2\frac{\Delta}{m_b} + \left[\left(\frac{1}{4}\ln\frac{m_b}{\mu} - \frac{11}{24}\right)\beta_0 + \left(\frac{5}{2} - \frac{\pi^2}{8}\right)C_F - \left(\frac{11}{48} - \frac{\pi^2}{16}\right)C_A\right]\ln\frac{\Delta}{m_b}$$
$$- \left(\frac{1}{2}\ln\frac{m_b}{\mu} - \frac{43}{96} - \frac{\pi^2}{48}\right)\beta_0 + \left(\frac{149}{48} + \frac{5\pi^2}{36} - \frac{9}{8}\,\zeta_3\right)C_F - \left(\frac{5}{16} + \frac{35\pi^2}{288} - \frac{9}{16}\,\zeta_3\right)C_A\,,$$
$$l_2(\Delta) = \left(\frac{\beta_0}{8} - \frac{4C_F}{9}\right)\ln^2\frac{\Delta}{m_b} + \left[\left(\frac{1}{6}\ln\frac{m_b}{\mu} - \frac{19}{72}\right)\beta_0 + \left(\frac{19}{18} - \frac{\pi^2}{12}\right)C_F - \left(\frac{11}{72} - \frac{\pi^2}{24}\right)C_A\right]\ln\frac{\Delta}{m_b}$$

$$
\begin{aligned}
&- \left(\frac{11}{36}\ln\frac{m_b}{\mu} - \frac{101}{432} - \frac{\pi^2}{72}\right)\beta_0 + \left(\frac{977}{432} + \frac{17\pi^2}{216} - \frac{3}{4}\,\zeta_3\right) C_F - \left(\frac{101}{432} + \frac{2\pi^2}{27} - \frac{3}{8}\,\zeta_3\right) C_A\,, \\
l_3(\Delta) = {}& \frac{C_F}{6}\ln^3\frac{\Delta}{m_b} + \left(\frac{2C_F}{9} + \frac{C_A}{16} - \frac{\beta_0}{16}\right)\ln^2\frac{\Delta}{m_b} \\
&+ \left[-\left(\frac{1}{12}\ln\frac{m_b}{\mu} - \frac{19}{144}\right)\beta_0 + \left(\frac{293}{144} + \frac{\pi^2}{36}\right) C_F + \left(\frac{11}{36} - \frac{\pi^2}{72}\right) C_A\right]\ln\frac{\Delta}{m_b} \\
&- \left(\frac{7}{72}\ln\frac{m_b}{\mu} + \frac{65}{864} + \frac{\pi^2}{144}\right)\beta_0 - \left(\frac{1451}{864} + \frac{11\pi^2}{216} - \frac{5}{12}\,\zeta_3\right) C_F + \left(\frac{149}{216} - \frac{13\pi^2}{432} - \frac{5}{24}\,\zeta_3\right) C_A\,.
\end{aligned}
\tag{41}
$$

This completes our compilation of theoretical formulae for the moments in the pole scheme. The first moment, $M_1(\Delta)$, and with it the average photon energy $\langle E_\gamma\rangle$, can be calculated including first- and second-order power corrections in the $1/m_b$ expansion. For the second moment, $M_2(\Delta)$, and hence for the variance σ_E^2, only first-order power corrections are available at present.

3.3 Elimination of pole-scheme parameters

It is well known that heavy-quark parameters defined in the pole scheme suffer from infrared renormalon ambiguities [30, 31, 32, 33]. As a result, the perturbative expansion for the moments presented in the previous section would not be well behaved. It is necessary to replace the pole mass m_b and other HQET parameters such as μ_π^2 in favor of some physical, short-distance quantities. For our purposes, the "shape-function scheme" proposed in [16] provides for a particularly suitable definition of the heavy-quark mass and kinetic energy. In this scheme, low-scale subtracted HQET parameters are defined via the moments of the renormalized shape function, regularized with a hard Wilsonian cutoff $\mu_f \gg \Lambda_{\rm QCD}$. In addition to their dependence on the cutoff, the HQET parameters depend on the scale μ at which the shape function is renormalized. For simplicity, we adopt the "diagonal" scale choice $\mu = \mu_f$. The conventional choice for the subtraction scale is $\mu_f = 1.5\,\text{GeV}$.

At two-loop order, the heavy-quark parameters $m_b(\mu_f)$ and $\mu_\pi^2(\mu_f)$ defined in the shape-function scheme are related to the pole-scheme parameters by [34, 35]

$$
\begin{aligned}
m_b\Big|_{\rm pole} = {}& m_b(\mu_f) + \mu_f\,\frac{C_F\alpha_s(\mu)}{\pi}\left\{1 + \frac{\alpha_s(\mu)}{\pi}\left[\left(\frac{1}{2}\ln\frac{\mu}{\mu_f} + \frac{47}{36}\right)\beta_0 + \left(\frac{23}{18} - \frac{\pi^2}{12} - \frac{9}{4}\,\zeta_3\right) C_A\right.\right. \\
&\left.\left. - \left(8 - \frac{\pi^2}{3} - 4\zeta_3\right) C_F\right]\right\} \\
&+ \frac{\mu_\pi^2(\mu_f)}{\mu_f}\,C_F\left(\frac{\alpha_s(\mu)}{\pi}\right)^2\left[-\frac{5\beta_0}{108} - \left(\frac{17}{54} - \frac{3}{4}\,\zeta_3\right) C_A + \left(1 - \frac{4}{3}\,\zeta_3\right) C_F\right] \\
&- \frac{\mu_f^2}{2m_b(\mu_f)}\,C_F\left(\frac{\alpha_s(\mu)}{\pi}\right)^2\left[-\frac{7\beta_0}{12} - \left(\frac{17}{12} - \frac{27}{8}\,\zeta_3\right) C_A + \left(\frac{27}{4} - 6\zeta_3\right) C_F\right] \\
&+ \frac{\mu_G^2 - \mu_\pi^2(\mu_f)}{2m_b(\mu_f)} + \dots\,,
\end{aligned}
$$

$$\mu_\pi^2\Big|_{\rm pole} = \mu_\pi^2(\mu_f)\left\{1 - \frac{C_F\alpha_s(\mu)}{2\pi} + C_F\left(\frac{\alpha_s(\mu)}{\pi}\right)^2\left[-\left(\frac{1}{4}\ln\frac{\mu}{\mu_f} - \frac{1}{8}\right)\beta_0 \right.\right.$$
$$\left.\left. + \left(\frac{5}{4} + \frac{\pi^2}{24} - \frac{27}{8}\,\zeta_3\right)C_A - \left(\frac{13}{4} + \frac{\pi^2}{6} - 6\zeta_3\right)C_F\right]\right\}$$
$$+ \mu_f^2\,C_F\left(\frac{\alpha_s(\mu)}{\pi}\right)^2\left[-\frac{7\beta_0}{12} - \left(\frac{17}{12} - \frac{27}{8}\,\zeta_3\right)C_A + \left(\frac{27}{4} - 6\zeta_3\right)C_F\right] + \dots\,. \qquad (42)$$

The analogous replacement rule for the parameter $\Delta = m_b - 2E_0$ follows from its definition. When these expressions are substituted for the pole-scheme parameters in the formulae for the moments, the results must be reexpanded consistently to the desired order in α_s and $1/m_b$. In the process, one finds that for the spectral moments in (5), the $1/m_b$-suppressed term in the replacement rule for the pole mass cancels against the contribution proportional to $(\mu_G^2 - \mu_\pi^2)$ from $M_1^{(1)}$ in (37). In the shape-function scheme, the predictions for $\langle E_\gamma\rangle$ and σ_E^2 are therefore independent of the parameter μ_G^2.

The arbitrary renormalization point μ of the running coupling $\alpha_s(\mu)$ in the relations (42) will be set equal to the matching scale μ_0 in all factorized, leading-power contributions. For the power corrections, where no scale separation is available, μ will be identified with the common renormalization scale in (37) and (38). The subtraction scale μ_f of the shape-function scheme is set by the upper limit on ω in shape-function integrals of the type (1). For the case of the $\bar B \to X_s\gamma$ moments this yields $\mu_f \sim \Delta \sim \mu_0$. Note that this implies a reshuffling between perturbative and non-perturbative terms at any given order in the $1/m_b$ expansion. For instance, eliminating the pole-scheme kinetic-energy parameter from the μ_π^2/Δ^2 power corrections in (26) adds terms of order $[\alpha_s(\mu_0)]^2$ to the leading-power contributions. As mentioned above, we will adopt the conventional choice $\mu_f = 1.5\,\text{GeV}$ in our numerical analysis, which is slightly larger than (but of the same magnitude as) the actual value $\Delta \approx 1\,\text{GeV}$.

While it is natural to use the shape-function scheme for analyses of inclusive B decays, this is by no means mandatory. In Appendix A.3, we present the corresponding replacement rules for the kinetic scheme introduced in [36]. We do not explore alternative short-distance definitions of the b-quark mass, such as the "$1S$ mass" [37] or the "potential-subtracted mass" [38]. The reason is that no physical definition of the kinetic-energy parameter μ_π^2 has been provided in these schemes, so they remove the renormalon problem only partially.

4 Boost to the $\Upsilon(4S)$ rest frame

Theoretical calculations of B-meson decay distributions are easiest to perform in the rest frame of the heavy meson. In all our results so far, E_γ denotes the photon energy measured in that frame. Existing experimental studies of the decay $\bar B \to X_s\gamma$ [19, 20, 21], however, measure the photon energy in a different frame. At an e^+e^- B-factory, pairs of $B\bar B$ mesons are produced on the $\Upsilon(4S)$ resonance peak. For CLEO, the $\Upsilon(4S)$ rest frame coincides with the laboratory system, whereas for BaBar and Belle the $\Upsilon(4S)$ rest frame can be constructed knowing the (asymmetric) energies of the electron and positron beams. In either case, the photon energy

is measured in the $\Upsilon(4S)$ rest frame, in which the B mesons have a small velocity

$$\beta = \sqrt{1 - \frac{4m_B^2}{m_{\Upsilon(4S)}^2}} \approx 0.064\,. \tag{43}$$

Below, we work out in detail how the properties of the photon spectrum and its moments are affected by boosting from the B-meson rest frame to the rest frame of the $\Upsilon(4S)$ resonance, following [7]. While this would be straightforward for moments of the entire spectrum, the presence of the cut leads to non-trivial complications. Note that future measurements of $\bar{B} \to X_s\gamma$ decay spectra relying on the full-reconstruction technique could reconstruct the B-meson rest frame and thus directly measure the spectrum in that reference system.

We denote quantities in the $\Upsilon(4S)$ rest frame with a prime. Let $k^\mu = E_\gamma(1, \boldsymbol{n})$ be the 4-vector of the photon in the B-meson rest frame. In the $\Upsilon(4S)$ system the B meson moves with velocity $\boldsymbol{\beta}$, and the photon energy is Doppler-shifted by an amount

$$E'_\gamma = E_\gamma \frac{1 - \boldsymbol{\beta}\cdot\boldsymbol{n}}{\sqrt{1-\beta^2}} = E_\gamma \frac{1 - \beta\cos\theta}{\sqrt{1-\beta^2}}\,, \tag{44}$$

where we have assumed without loss of generality that $\boldsymbol{\beta}$ points in the z-direction. The photon spectrum dN/dE'_γ in the $\Upsilon(4S)$ rest frame can be obtained in terms of the spectrum dN/dE_γ in the B-meson rest frame by evaluating

$$\begin{aligned}\frac{dN}{dE'_\gamma} &= \int \frac{d\phi\, d\cos\theta}{4\pi} \int dE_\gamma \frac{dN}{dE_\gamma}\, \delta\Big(E'_\gamma - E_\gamma \frac{1-\beta\cos\theta}{\sqrt{1-\beta^2}}\Big) \\ &= \frac{1}{\beta_+ - \beta_-} \int\limits_{\beta_- E'_\gamma}^{\min(\beta_+ E'_\gamma, E_\gamma^{\max})} dE_\gamma \frac{1}{E_\gamma} \frac{dN}{dE_\gamma}\,,\end{aligned} \tag{45}$$

where $\beta_\pm = \sqrt{(1\pm\beta)/(1\mp\beta)}$. This reproduces eq. (B.1) in [7].

It is now straightforward to compute the effect of the boost on moments of the photon spectrum. We obtain

$$\begin{aligned}\int\limits_{E_0}^{E_\gamma'^{\max}} dE'_\gamma\, (E'_\gamma)^n \frac{dN}{dE'_\gamma} &= \frac{\beta_+^{n+1} - \beta_-^{n+1}}{(n+1)(\beta_+ - \beta_-)} \int\limits_{E_0}^{E_\gamma^{\max}} dE_\gamma\, (E_\gamma)^n \frac{dN}{dE_\gamma} \\ &+ \frac{1}{(n+1)(\beta_+ - \beta_-)} \left[\int\limits_{\beta_- E_0}^{E_0} dE_\gamma \frac{1}{E_\gamma} \frac{dN}{dE_\gamma} \Big[(\beta_+ E_\gamma)^{n+1} - (E_0)^{n+1}\Big] - (\beta_+ \leftrightarrow \beta_-) \right],\end{aligned} \tag{46}$$

where $E_\gamma'^{\max} = \beta_+ E_\gamma^{\max}$, and the same value of the cutoff E_0 must be used on both sides of the equation. In order to illustrate the effect of the boost on the moments, we use the theoretical description of the $\bar{B} \to X_s\gamma$ photon spectrum at NLO presented in [35] to generate the distribution dN/dE_γ in the B-meson rest frame. We adopt the default choices for all parameters and use two models of the shape function, corresponding to heavy-quark parameters

Table 1: Predictions for the average photon energy and the variance of the photon spectrum in the B-meson and $\Upsilon(4S)$ rest frames, for different values of the cutoff E_0. In each case, the first line refers to shape-function model 1, the second line to model 2. See text for explanation.

	$\langle E_\gamma\rangle$ [GeV]		σ_E^2 [$10^{-2}\,\text{GeV}^2$]	
E_0 [GeV]	B frame	$\Upsilon(4S)$ frame	B frame	$\Upsilon(4S)$ frame
1.8	2.311	2.317	3.10	3.76
	2.286	2.292	3.73	4.35
1.9	2.325	2.331	2.54	3.17
	2.305	2.313	3.01	3.59
2.0	2.341	2.350	1.99	2.59
	2.329	2.338	2.31	2.87

$m_b(\mu_f) = 4.61\,\text{GeV}$, $\mu_\pi^2(\mu_f) = 0.2\,\text{GeV}^2$ (model 1) and $m_b(\mu_f) = 4.55\,\text{GeV}$, $\mu_\pi^2(\mu_f) = 0.3\,\text{GeV}^2$ (model 2) at $\mu_f = 1.5\,\text{GeV}$. In Table 1, we compare the results for the average photon energy and the variance of the spectrum in the B-meson and $\Upsilon(4S)$ rest frames. Numerically, it turns out that the terms containing the cutoff E_0 in (46) have a small effect. Keeping only the contribution in the first line of that equation (corresponding to the limit where $E_0 = 0$) yields the simple relations

$$\begin{aligned}\langle E'_\gamma\rangle - \langle E_\gamma\rangle &= \left(\frac{1}{\sqrt{1-\beta^2}} - 1\right)\langle E_\gamma\rangle \approx 0.005\,\text{GeV}\,,\\ \sigma^2_{E'} - \sigma^2_E &= \frac{\beta^2}{3(1-\beta^2)}\left[\langle E_\gamma\rangle^2 + 4\sigma_E^2\right] \approx 0.007\,\text{GeV}^2\,.\end{aligned} \tag{47}$$

This explains to a large extent the shifts seen in the table.

5 Numerical analysis

The theoretical expressions for the spectral moments depend on several input parameters, whose values are summarized in Table 2. The relevant hadronic parameters are μ_π^2, ρ_D^3, ρ_{LS}^3, and μ_G^2 if the kinetic scheme is used instead of the shape-function scheme. As mentioned earlier, at tree level the results for the spectral moments are $\langle E_\gamma\rangle = m_b/2 + \ldots$ and $\sigma_E^2 = \mu_\pi^2/12 + \ldots$, and our goal will be to determine the parameters (m_b, μ_π^2) from a fit to experimental data. The sensitivity of the moments to other hadronic parameters is very weak (see below), so it is safe to use them as fixed inputs in the fit. Following [39], we define the quantities ρ_D^3 and ρ_{LS}^3 in the pole scheme, which is justified given the smallness of their contributions to the moments. We use as inputs the values $\rho_D^3 = (0.195 \pm 0.029)\,\text{GeV}^3$ and $\rho_{LS}^3 = (-0.085 \pm 0.082)\,\text{GeV}^3$ extracted

Table 2: Compilation of input parameters.

Parameter	Value
ρ_D^3	$(0.11 \pm 0.05)\,\text{GeV}^3$
ρ_{LS}^3	$(-0.09 \pm 0.08)\,\text{GeV}^3$
μ_G^2	$(0.35 \pm 0.07)\,\text{GeV}^2$
m_c/m_b	0.222 ± 0.030
m_s/m_b	0.02
$\alpha_s(m_Z)$	0.1187

from a global fit to $\bar{B} \to X_c\, l^- \bar{\nu}$ moments in the kinetic scheme [1] and convert them to the pole scheme by subtracting $[2C_F\alpha_s(2\mu_f)/3\pi]\,\mu_f^3 \approx 0.09\,\text{GeV}^3$ (at $\mu_f = 1\,\text{GeV}$) from ρ_D^3 [36]. We inflate the error on ρ_D^3 from 0.03 to $0.05\,\text{GeV}^3$ to be conservative. The resulting values are consistent with, but more accurate than, the theoretical estimates $\rho_D^3 = (0.1 \pm 0.1)\,\text{GeV}^3$ and $\rho_{LS}^3 = (-0.15 \pm 0.10)\,\text{GeV}^3$ given in [36, 40]. The value for ρ_D^3 is also in agreement with early estimates using the vacuum-insertion approximation, which gave $\rho_D^3 \approx (2\pi\alpha_s/9)\, f_B^2 m_B \approx 0.1\,\text{GeV}^3$ [11, 41]. The value of μ_G^2 quoted in the table is derived using (35) and assigning an error for possible $1/m_b$ corrections [40]. The formulae for the power corrections to the moments involve numerically small terms depending on the quark-mass ratios $z = (m_c/m_b)^2$ and m_s/m_b, for which we adopt values consistent with [15]. Throughout, we use the three-loop running coupling constant, matched to a four-flavor theory at $\mu = \overline{m}_b(\overline{m}_b) = 4.25\,\text{GeV}$.

Because of the truncation of perturbation theory, our results are sensitive to the choice of the various factorization scales. This sensitivity can be taken as an estimator of the residual perturbative uncertainty. In the resummed expressions obtained in RG-improved perturbation theory, we vary the three matching scales by a factor between $1/\sqrt{2}$ and $\sqrt{2}$ about their default values $\mu_h^{\text{def}} = m_b$, $\mu_i^{\text{def}} = \sqrt{m_b\Delta}$, and $\mu_0^{\text{def}} = \Delta$, using $m_b = 4.65\,\text{GeV}$ as a reference value. The scale μ in the expressions for the power corrections is set equal to μ_i but varied independently. Thus, for $E_0 = 1.8\,\text{GeV}$ we vary $\mu_h \in [3.29, 6.58]\,\text{GeV}$, $\mu_i, \mu \in [1.56, 3.12]\,\text{GeV}$, and $\mu_0 \in [0.74, 1.48]\,\text{GeV}$. Together this covers a conservative range of scales. When quoting results in fixed-order perturbation theory (in which all scales are set equal to μ), we vary μ between 1 and 5 GeV.

5.1 Predictions for the moments of the photon spectrum

We begin by presenting predictions for the average photon energy and the variance of the photon spectrum, including a detailed account of theoretical uncertainties. We define the heavy-quark parameters m_b and μ_π^2 in the shape-function scheme at a subtraction point $\mu_f = 1.5\,\text{GeV}$. For reference, we recall that the values for these parameters extracted from a global fit to $\bar{B} \to X_c\, l^- \bar{\nu}$ moments are $m_b = (4.61 \pm 0.08)\,\text{GeV}$ and $\mu_\pi^2 = (0.15 \pm 0.07)\,\text{GeV}^2$ [34], where we account for the small $1/m_b$ corrections in the relation for the pole mass in (42),

Table 3: Predictions and error analysis for the first two moments of the photon spectrum, defined with a cutoff $E_0 = 1.8\,\text{GeV}$. The parameters $m_b = 4.61\,\text{GeV}$ and $\mu_\pi^2 = 0.15\,\text{GeV}^2$ are kept fixed. In each column, the upper (lower) error indicates the variation obtained by increasing (decreasing) a given input parameter.

Moment	Value	μ_0	μ_i	μ_h	μ	m_c/m_b	ρ_D^3	ρ_{LS}^3
$\langle E_\gamma\rangle$ $[10^{-3}\,\text{GeV}]$	2287	$^{-\ 1}_{+22}$	$^{-11}_{+\ 7}$	∓ 1	$^{+5}_{-7}$	$^{+2}_{-1}$	∓ 1	± 2
σ_E^2 $[10^{-4}\,\text{GeV}^2]$	334	$^{+15}_{-84}$	$^{-26}_{+47}$	± 2	$^{-11}_{+12}$	$^{-4}_{+3}$	∓ 18	± 14

which were not included in that paper. For the purpose of illustration, we use the central values of these parameters for the following discussion.

The predictions for the average photon energy and variance are obtained using the relations in (5). In calculating $\langle E_\gamma\rangle$, we include both first- and second-order power corrections to the moment M_1, as given in Section 3. When calculating the variance, we use the second relation in (5) and compute, for consistency, all quantities (M_1, M_2, and $\langle E_\gamma\rangle$) including first-order power corrections. Table 3 shows our results for the case $E_0 = 1.8\,\text{GeV}$, corresponding to the lowest value of the cutoff that has so far been achieved experimentally [20]. As expected, the perturbative uncertainties are larger the smaller the relevant matching scales are, but they remain under good control even for the lowest scale μ_0. The sensitivity to other input parameters, and in particular to the hadronic quantities ρ_D^3 and ρ_{LS}^3, is very small. The convergence of the heavy-quark expansion is good for both moments. The first-order power correction to the average photon energy lowers the value of $\langle E_\gamma\rangle$ by about 54 MeV, corresponding to an 11% reduction of the difference $(\langle E_\gamma\rangle - E_0)$, which is the relevant quantity to compare with. The impact of the second-order power correction is negligible (+2 MeV, corresponding to a 0.4% increase). The first-order power correction to the second moment is larger and constitutes about 27% of the total value. The main effect is due to the first-order correction to $\langle E_\gamma\rangle$, which enters via the second term in the relation for the variance in (5).

Next, we study the behavior of the perturbative expansions of the moments and explore to what extent it is improved by using scale separation and RG improvement, which is one of the main new features of our approach. Figure 1 shows our predictions for the average photon energy and variance, using both RG-improved and fixed-order perturbation theory. In each plot the solid, dashed, and dotted curves correspond to the NNLO ($\sim\alpha_s^2$), NLO ($\sim\alpha_s$), and LO ($\sim\alpha_s^0$) approximations, respectively. In the factorized expressions, the four relevant scales ($\mu_n = \mu_h, \mu_i, \mu_0, \mu$) are varied simultaneously (and in a correlated way) about their default values (μ_n^{def}). We observe an excellent stability of the RG-improved results under scale variation, both at NLO and NNLO. In the case of fixed-order perturbation theory, on the other hand, the results obtained at NNLO are less stable than those obtained at NLO (the tree-level LO results are trivially scale independent in fixed-order calculations). While the absolute variations are still modest for the average photon energy, they are quite large for the case of the variance. We conclude that a proper scale separation is important for obtaining

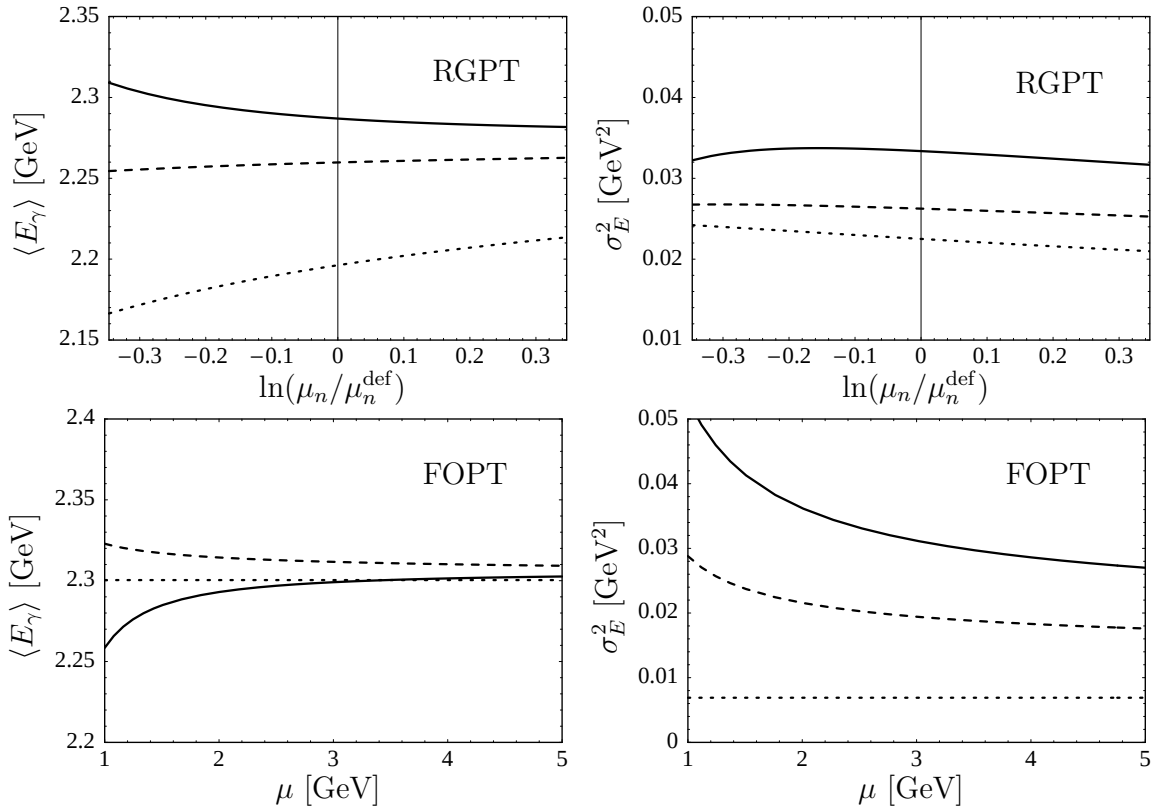

Figure 1: Scale dependence of the predictions for the first two moments of the photon spectrum, defined with a cut at $E_0 = 1.8\,\text{GeV}$ in the B-meson rest frame, in RG-improved perturbation theory (RGPT, top) and fixed-order perturbation theory (FOPT, bottom). Solid, dashed, and dotted lines refer to the NNLO, NLO, and LO approximations. All parameters are set to their default values.

reliable perturbative predictions for the moments.

In order to obtain a more conservative estimate of the remaining perturbative uncertainty, one should vary the different scales entering the RG-improved expressions independently. This is done in Figure 2, where we explore the sensitivity to variations of the individual matching scales on an expanded scale. The underlaid gray bands indicate the total perturbative errors we assign. They are obtained by combining the various variations in quadrature, ignoring however very low values of the soft scale μ_0, where $\alpha_s(\mu_0)$ is so large that perturbation theory deteriorates. Combining also the parametric uncertainties in quadrature, and allowing for small variations of m_b and μ_π^2 about their default values, we obtain for $E_0 = 1.8\,\text{GeV}$

$$\begin{aligned}\langle E_\gamma \rangle &= (2.287 \pm 0.013_{\rm pert} \pm 0.003_{\rm pars})\,\text{GeV} + 0.44\,\delta m_b + 0.010\,\text{GeV}^{-1}\,\delta\mu_\pi^2\,,\\ \sigma_E^2 &= (0.0334 \pm 0.0051_{\rm pert} \pm 0.0023_{\rm pars})\,\text{GeV}^2 + 0.020\,\text{GeV}\,\delta m_b + 0.073\,\delta\mu_\pi^2\,. \end{aligned} \tag{48}$$

The central values are in excellent agreement with the results found by the Belle Collaboration [20] and collected in Table 4. This indicates that the values for m_b and μ_π^2 extracted from $\bar{B} \to X_c\, l^-\bar{\nu}$ moment fits are compatible with those favored by the $\bar{B} \to X_s\gamma$ photon spectrum,

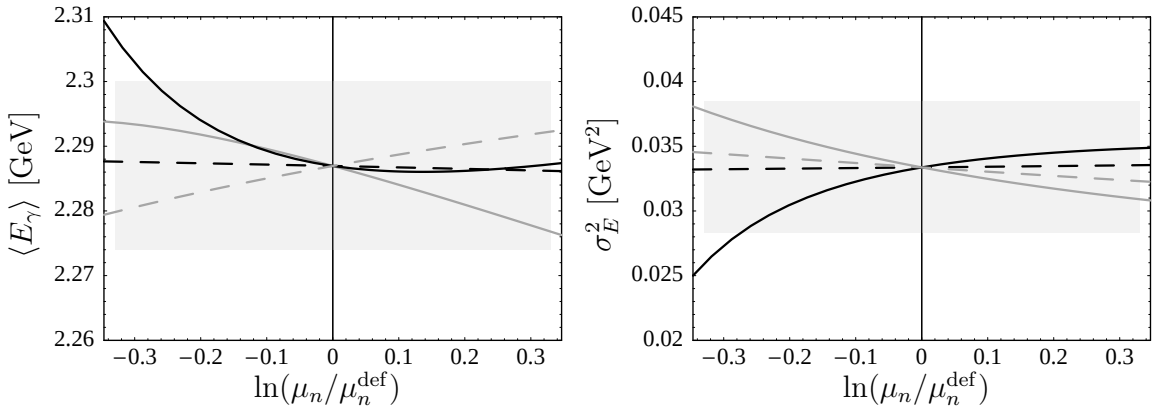

Figure 2: Scale dependence of the predictions for the first two moments of the photon spectrum in RG-improved perturbation theory: variation of μ_0 (solid), variation of μ_i (solid gray), variation of μ_h (dashed), variation of μ (dashed gray). The light shaded areas show the estimated perturbative uncertainties.

Table 4: Experimental results for the first two moments of the $\bar{B} \to X_s\gamma$ photon spectrum, defined with a cut $E_\gamma \geq E_0$. All results refer to the B-meson rest frame.

E_0 [GeV]	$\langle E_\gamma \rangle$ [GeV]	σ_E^2 [$10^{-2}\,\text{GeV}^2$]	Reference
1.8	$2.292 \pm 0.027 \pm 0.033$	$3.05 \pm 0.79 \pm 0.99$	Belle [20]
1.9	$2.321 \pm 0.038^{+0.017}_{-0.038}$	$2.53 \pm 1.01^{+0.41}_{-0.28}$	BaBar [21]
2.0	$2.346 \pm 0.032 \pm 0.011$	$2.26 \pm 0.66 \pm 0.20$	CLEO [19]

which by itself is a non-trivial test of the heavy-quark expansion. Note that the theoretical error estimates are in agreement with the naive estimates presented at the end of Section 2.1. It follows from the first relation that the b-quark mass can be extracted with exquisitely small theoretical uncertainties of only $(\pm 29_{\rm pert} \pm 6_{\rm pars})\,\text{MeV}$ form the average photon energy. From the second moment, the combination $\mu_\pi^2 + 0.27\,\text{GeV}\,m_b$ can be extracted with errors of $(\pm 0.07_{\rm pert} \pm 0.03_{\rm pars})\,\text{GeV}^2$. Given the precision achieved on m_b, these errors essentially determine the precision on the extraction of the parameter μ_π^2.

The precision achieved for the mass determination profits greatly from the availability of a complete NNLO prediction for the first moment. If we used instead only the NLO approximation, the combined perturbative error on $\langle E_\gamma \rangle$ would increase from $\pm 13\,\text{MeV}$ to $\pm 40\,\text{MeV}$, yielding a theory error of about $\pm 100\,\text{MeV}$ (from perturbation theory) on the extracted value for m_b, in agreement with the findings of [15].

The above analysis can be repeated for other values of the cutoff E_0, however only within certain limits. The default value for the soft scale, $\mu_0 = \Delta = m_b - 2E_0$, is $0.85\,\text{GeV}$ for $E_0 = 1.9\,\text{GeV}$ (as used in the BaBar analysis in [21]), and $0.65\,\text{GeV}$ for $E_0 = 2.0\,\text{GeV}$ (as employed in the CLEO analysis in [19]). In the latter case a short-distance treatment cannot

reasonably be expected to work, and one should resort to a description in terms of shape functions, such as [7, 35]. For $E_0 = 1.9\,\text{GeV}$ the applicability of our approach is marginal, and indeed plots analogous to Figure 2 exhibit a more pronounced sensitivity to variations of the low scale μ_0 in this case. Accounting for this by a 50% increase of the perturbative error, we find

$$\begin{aligned}\langle E_\gamma\rangle &= (2.305 \pm 0.020_{\rm pert} \pm 0.003_{\rm pars})\,\text{GeV} + 0.43\,\delta m_b + 0.016\,\text{GeV}^{-1}\,\delta\mu_\pi^2\,,\\ \sigma_E^2 &= (0.0302 \pm 0.0077_{\rm pert} \pm 0.0023_{\rm pars})\,\text{GeV}^2 + 0.012\,\text{GeV}\,\delta m_b + 0.071\,\delta\mu_\pi^2\,. \end{aligned} \tag{49}$$

These theoretical results are in good agreement with the moment measurements reported by the BaBar Collaboration [21].

5.2 Combined moment fits

We are now ready to perform a combined analysis of the experimental data for the first two moments of the $\bar B \to X_s\gamma$ photon spectrum with the goal to extract the values of the heavy-quark parameters m_b and μ_π^2. To this end, we define

$$\chi^2(m_b,\mu_\pi^2) = \sum_{i,j=1,2} (X_i^{\rm exp} - X_i^{\rm th})\,(V^{-1})_{ij}\,(X_j^{\rm exp} - X_j^{\rm th})\,, \tag{50}$$

where $X_1 = \langle E_\gamma\rangle$ and $X_2 = \sigma_E^2$ are the two observables, and V is the covariance matrix containing information about the errors and correlations in the measurements of these two quantities [20, 21]. In the theoretical calculation of $X_i^{\rm th}$ we keep all theory parameters other than m_b and μ_π^2 fixed to their default values. Throughout, we use expressions in RG-improved perturbation theory. For a given set of measurements, the point where $\chi^2 = 0$ determines the best fit values. Figure 3 shows contours of $\chi^2 = 1$ and $\chi^2 = 2.69$ in the m_b–μ_π^2 plane obtained by fitting the data of the Belle and BaBar Collaborations. We show results for the shape-function scheme considered so far, as well as for the kinetic scheme (see Appendix A.3), which has been used, e.g., in the $\bar B \to X_c\,l^-\bar\nu$ moment analysis in [1]. The solid contours refer to the NNLO formulae derived in the present work, while the dashed contours correspond to the NLO approximation. The NLO results are consistent with those obtained at NNLO when one takes into account theoretical uncertainties, which are much larger at NLO.

Adding the theoretical uncertainties as determined in the previous section (errors for the kinetic scheme are determined in an analogous way), we find

$$\begin{aligned} m_b^{\rm SF} &= (4.622 \pm 0.099_{\rm exp} \pm 0.030_{\rm th})\,\text{GeV}\,, \quad \mu_\pi^{2,\rm SF} = (0.108 \pm 0.186_{\rm exp} \pm 0.077_{\rm th})\,\text{GeV}^2\,,\\ m_b^{\rm kin} &= (4.543 \pm 0.114_{\rm exp} \pm 0.041_{\rm th})\,\text{GeV}\,, \quad \mu_\pi^{2,\rm kin} = (0.495 \pm 0.176_{\rm exp} \pm 0.085_{\rm th})\,\text{GeV}^2\,, \end{aligned} \tag{51}$$

from the fit to the Belle data [20], and

$$\begin{aligned} m_b^{\rm SF} &= (4.648 \pm 0.111_{\rm exp} \pm 0.047_{\rm th})\,\text{GeV}\,, \quad \mu_\pi^{2,\rm SF} = (0.076 \pm 0.161_{\rm exp} \pm 0.113_{\rm th})\,\text{GeV}^2\,,\\ m_b^{\rm kin} &= (4.556 \pm 0.117_{\rm exp} \pm 0.060_{\rm th})\,\text{GeV}\,, \quad \mu_\pi^{2,\rm kin} = (0.522 \pm 0.143_{\rm exp} \pm 0.122_{\rm th})\,\text{GeV}^2\,, \end{aligned} \tag{52}$$

from the fit to the BaBar data [21]. The fits to the two data sets are consistent with each other, but the theoretical errors are smaller in the first case due to the lower value of E_0 used

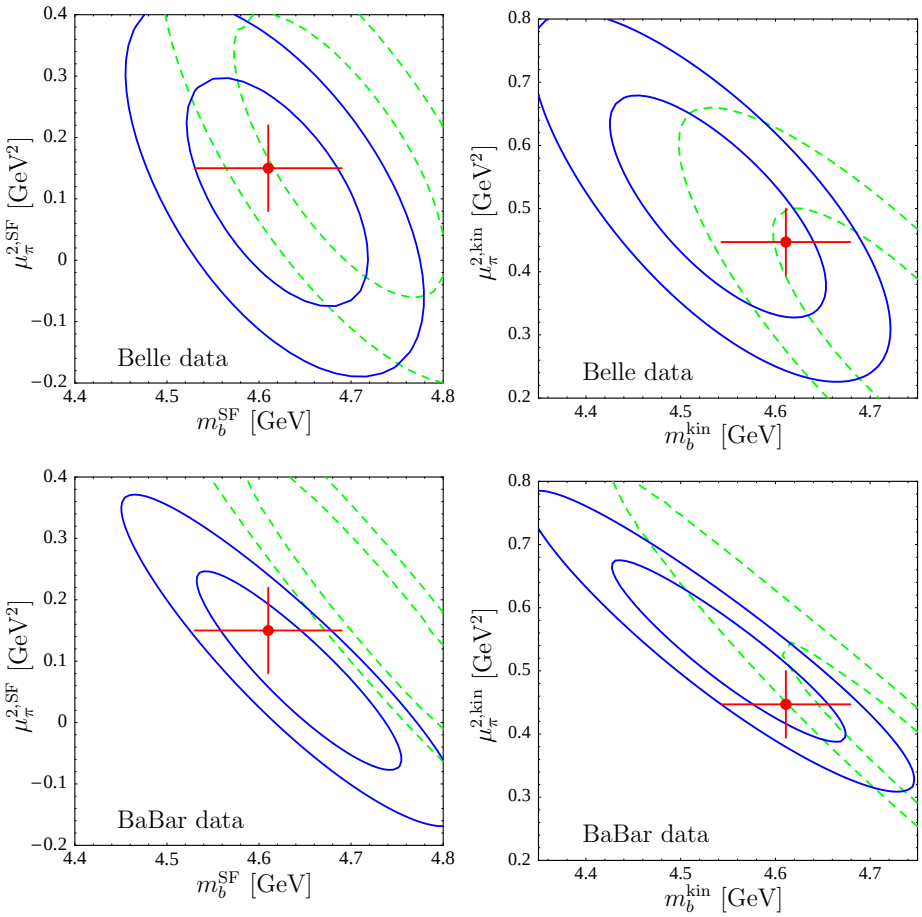

Figure 3: Fits to the Belle and BaBar data for the moments of the photon spectrum. We show contours where $\chi^2 = 1$ and 2.69, so that projections onto the axes yield parameter ranges at 68% and 90% confidence level. The fits are performed using the shape-function scheme (left) and the kinetic scheme (right). The solid (dashed) contour lines refer to the NNLO (NLO) approximation. The points with error bars indicate the results obtained from the $\bar{B} \to X_c\, l^-\bar{\nu}$ moment analysis.

in the Belle analysis. In the shape-function scheme m_b and μ_π^2 are defined at $\mu_f = 1.5\,\mathrm{GeV}$, while in the kinetic scheme we adopt the conventional choice $\mu_f = 1\,\mathrm{GeV}$. In all cases there is a strong anti-correlation of the two quantities, as can be seen from the figure.

The values for the heavy-quark parameters determined form the fit to the $\bar{B} \to X_s\gamma$ moments are in excellent agreement with those derived from moments in $\bar{B} \to X_c\, l^-\bar{\nu}$ decays, which are $m_b^{\mathrm{SF}} = (4.61 \pm 0.08)\,\mathrm{GeV}$ and $\mu_\pi^{2,\mathrm{SF}} = (0.15 \pm 0.07)\,\mathrm{GeV}^2$ in the shape-function scheme [34], and $m_b^{\mathrm{kin}} = (4.611 \pm 0.068)\,\mathrm{GeV}$ and $\mu_\pi^{2,\mathrm{kin}} = (0.447 \pm 0.053)\,\mathrm{GeV}^2$ in kinetic scheme [1]. These reference values are shown as data points in Figure 3 for comparison. The combined average values obtained from (51) and (52) are $m_b^{\mathrm{SF}} = (4.63 \pm 0.08)\,\mathrm{GeV}$ and $\mu_\pi^{2,\mathrm{SF}} = (0.09 \pm 0.14)\,\mathrm{GeV}^2$, and $m_b^{\mathrm{kin}} = (4.55 \pm 0.09)\,\mathrm{GeV}$ and $\mu_\pi^{2,\mathrm{kin}} = (0.51 \pm 0.14)\,\mathrm{GeV}^2$. However, given that the BaBar data are still preliminary and that they employ a higher value of E_0, we consider the fit to the Belle data as our most reliable result. Combining the values

in (51) with the ones extracted from the $\bar{B} \to X_c\, l^- \bar{\nu}$ moment fit yields

$$\begin{aligned} m_b^{\rm SF} &= (4.61 \pm 0.06)\,{\rm GeV}\,, \qquad \mu_\pi^{2,{\rm SF}} = (0.15 \pm 0.07)\,{\rm GeV}^2\,, \\ m_b^{\rm kin} &= (4.59 \pm 0.06)\,{\rm GeV}\,, \qquad \mu_\pi^{2,{\rm kin}} = (0.45 \pm 0.05)\,{\rm GeV}^2\,. \end{aligned} \tag{53}$$

6 Conclusions

Moments of the photon energy spectrum in the inclusive radiative decay $\bar{B} \to X_s\gamma$ are sensitive probes of low-scale hadronic dynamics. They can be used to extract accurate values for the b-quark mass and the kinetic-energy parameter μ_π^2 of heavy-quark effective theory. Starting from an exact QCD factorization formula for the partial $\bar{B} \to X_s\gamma$ decay rate, we have derived improved predictions for the first two moments, $\langle E_\gamma\rangle$ and $\langle E_\gamma^2\rangle - \langle E_\gamma\rangle^2$, defined with a cut $E_\gamma \geq E_0$ on the photon energy. In the region where $\Delta = m_b - 2E_0$ is large compared with $\Lambda_{\rm QCD}$, a theoretical description without recourse to shape (or bias) functions has been achieved.

The leading terms in the $1/m_b$ expansion of the moments receive contributions from the low and intermediate scales Δ and $\sqrt{m_b\Delta}$, but not from the hard scale m_b. For these terms, a complete scale separation is achieved at next-to-next-to-leading order (NNLO) in renormalization-group improved perturbation theory, including two-loop matching contributions and three-loop running. Given that $\Delta \approx 1\,{\rm GeV}$ is a rather low scale, it is not surprising that the NNLO perturbative corrections are numerically significant. They lead to significant shifts in the central values of the heavy-quark parameters m_b and μ_π^2 extracted from a fit to experimental data for the first two moments. When the different scales are properly separated using renormalization-group techniques, the inclusion of the NNLO corrections helps reducing the residual scale uncertainties in the theoretical predictions. This allows us to extract the heavy-quark parameters with excellent theoretical accuracy, namely $\delta m_b = 30\,{\rm MeV}$ and $\delta\mu_\pi^2 = 0.08\,{\rm GeV}^2$. The extracted values are in very good agreement with those derived from moments of inclusive $\bar{B} \to X_c\, l^- \bar{\nu}$ decay distributions. This agreement is gratifying given the different nature of the theoretical framework used to analyze these two classes of decays: a conventional operator product expansion in the case of $\bar{B} \to X_c\, l^- \bar{\nu}$ decay, and QCD factorization in the case of $\bar{B} \to X_s\gamma$.

As the data on the $\bar{B} \to X_s\gamma$ photon spectrum will become more accurate in the near future, the tools developed in this work will enable us to determine the b-quark mass with unprecedented precision. This, in turn, will help to reduce the theoretical uncertainties in the determination of $|V_{ub}|$ using, e.g., the approach of [35].

Acknowledgments: I am grateful to Thomas Becher, Richard Hill, Björn Lange, and Gil Paz for several useful discussions, to Nikolai Uraltsev for clarifications concerning the kinetic scheme, and to Francesca Di Lodovico, Henning Flaecher, and Antonio Limosani for communications concerning the BaBar and Belle data. I wish to thank the Institute for Advanced Study (Princeton, NJ) for hospitality and support as a member for the fall term 2004, during which most of this work was completed. This research was supported by the National Science Foundation under Grant PHY-0355005, and by the Department of Energy under Grant DE-FG02-90ER40542.

Appendices

A.1 Perturbative expansion of η

The expansion of the parameter η defined in (7) in RG-improved perturbation theory can be derived using the perturbative expansions of the cusp anomalous dimension and β function, which we write as

$$\Gamma_{\rm cusp}(\alpha_s) = \sum_{n=0}^{\infty} \Gamma_n \left(\frac{\alpha_s}{4\pi}\right)^{n+1}, \qquad \beta(\alpha_s) = \frac{d\alpha_s}{d\ln\mu} = -2\alpha_s \sum_{n=0}^{\infty} \beta_n \left(\frac{\alpha_s}{4\pi}\right)^{n+1}. \tag{54}$$

At NNLO, we obtain

$$\begin{aligned}\eta = \frac{\Gamma_0}{\beta_0}\Bigg\{ &\ln\frac{\alpha_s(\mu_0)}{\alpha_s(\mu_i)} + \left(\frac{\Gamma_1}{\Gamma_0} - \frac{\beta_1}{\beta_0}\right)\frac{\alpha_s(\mu_0)-\alpha_s(\mu_i)}{4\pi} \\ &+ \left[\frac{\Gamma_2}{\Gamma_0} - \frac{\beta_2}{\beta_0} - \frac{\beta_1}{\beta_0}\left(\frac{\Gamma_1}{\Gamma_0} - \frac{\beta_1}{\beta_0}\right)\right]\frac{\alpha_s^2(\mu_0)-\alpha_s^2(\mu_i)}{32\pi^2} + \dots\Bigg\}. \end{aligned} \tag{55}$$

The expansion coefficients of the β function to three-loop order in the $\overline{\rm MS}$ scheme are [42]

$$\begin{aligned}\beta_0 &= \frac{11}{3}\,C_A - \frac{2}{3}\,n_f\,, \qquad \beta_1 = \frac{34}{3}\,C_A^2 - \frac{10}{3}\,C_A\,n_f - 2C_F\,n_f\,, \\ \beta_2 &= \frac{2857}{54}\,C_A^3 + \left(C_F^2 - \frac{205}{18}\,C_F C_A - \frac{1415}{54}\,C_A^2\right)n_f + \left(\frac{11}{9}\,C_F + \frac{79}{54}\,C_A\right)n_f^2\,. \end{aligned} \tag{56}$$

The three-loop expression for the cusp anomalous dimension has recently been obtained in [43]. The expansion coefficients are

$$\begin{aligned}\Gamma_0 &= 4C_F\,, \qquad \Gamma_1 = C_F\left[\left(\frac{268}{9} - \frac{4\pi^2}{3}\right)C_A - \frac{40}{9}\,n_f\right], \\ \Gamma_2 &= 16C_F\Bigg[\left(\frac{245}{24} - \frac{67\pi^2}{54} + \frac{11\pi^4}{180} + \frac{11}{6}\,\zeta_3\right)C_A^2 - \left(\frac{209}{108} - \frac{5\pi^2}{27} + \frac{7}{3}\,\zeta_3\right)C_A\,n_f \\ &\quad - \left(\frac{55}{24} - 2\zeta_3\right)C_F\,n_f - \frac{n_f^2}{27}\Bigg]. \end{aligned} \tag{57}$$

A.2 Perturbative expansions of the jet and soft functions

The two-loop matching conditions at the hard-collinear and soft scales are encoded in the functions j and s defined in (8) and (11), respectively. At two-loop order, explicit expressions for these quantities have been given in (23). Besides the expansion coefficients of the β function and cusp anomalous dimension, the results involve the one- and two-loop coefficients of anomalous dimensions γ and γ^J, which we define as

$$\gamma^{(J)}(\alpha_s) = \sum_{n=0}^{\infty} \gamma_n^{(J)} \left(\frac{\alpha_s}{4\pi}\right)^{n+1}. \tag{58}$$

The two-loop coefficient of the anomalous dimension γ entering the shape-function evolution kernel has been calculated long ago in [44], and some errors in this calculation have now been corrected [15, 45] (see also the Erratum to [44]). The result is

$$\gamma_0 = -2C_F\,, \qquad \gamma_1 = C_F\left[\left(\frac{110}{27}+\frac{\pi^2}{18}-18\zeta_3\right)C_A+\left(\frac{4}{27}+\frac{\pi^2}{9}\right)n_f\right]. \tag{59}$$

The two-loop anomalous dimension γ^J of the jet function in soft-collinear effective theory (SCET) has not yet been computed directly. A calculation is in progress and has already led to a prediction for the terms of order $C_F n_f$ [46]. The remaining terms can be deduced by noting that the SCET jet function is related to the familiar jet function from deep-inelastic scattering. The result is [15]

$$\begin{aligned}\gamma_0^J &= -3C_F\,,\\ \gamma_1^J &= C_F\left[-\left(\frac{3}{2}-2\pi^2+24\zeta_3\right)C_F-\left(\frac{1769}{54}+\frac{11\pi^2}{9}-40\zeta_3\right)C_A+\left(\frac{121}{27}+\frac{2\pi^2}{9}\right)n_f\right].\end{aligned} \tag{60}$$

A.3 Heavy-quark parameters in the kinetic scheme

The defining relations for the b-quark mass and kinetic-energy parameter in the kinetic scheme are [36]

$$\begin{aligned} m_b\Big|_{\rm pole} &= m_b(\mu_f)+\frac{4}{3}\,\mu_f\,\frac{C_F\alpha_s(\mu)}{\pi}\left\{1+\frac{\alpha_s(\mu)}{\pi}\left[\left(\frac{1}{2}\ln\frac{\mu}{2\mu_f}+\frac{4}{3}\right)\beta_0+\left(\frac{13}{12}-\frac{\pi^2}{6}\right)C_A\right]\right\}\\ &\quad+\frac{\mu_f^2}{2m_b(\mu_f)}\,\frac{C_F\alpha_s(\mu)}{\pi}\left\{1+\frac{\alpha_s(\mu)}{\pi}\left[\left(\frac{1}{2}\ln\frac{\mu}{2\mu_f}+\frac{13}{12}\right)\beta_0+\left(\frac{13}{12}-\frac{\pi^2}{6}\right)C_A\right]\right\}+\dots\,,\\ \mu_\pi^2\Big|_{\rm pole} &= \mu_\pi^2(\mu_f)-\mu_f^2\,\frac{C_F\alpha_s(\mu)}{\pi}\left\{1+\frac{\alpha_s(\mu)}{\pi}\left[\left(\frac{1}{2}\ln\frac{\mu}{2\mu_f}+\frac{13}{12}\right)\beta_0+\left(\frac{13}{12}-\frac{\pi^2}{6}\right)C_A\right]\right\}+\dots\,. \end{aligned} \tag{61}$$

The conventional choice for the subtraction scale is $\mu_f = 1\,\text{GeV}$.

References

[1] B. Aubert *et al.* [BaBar Collaboration], Phys. Rev. Lett. **93**, 011803 (2004) [hep-ex/0404017].

[2] C. W. Bauer, Z. Ligeti, M. Luke, A. V. Manohar and M. Trott, Phys. Rev. D **70**, 094017 (2004) [hep-ph/0408002].

[3] A. Kapustin and Z. Ligeti, Phys. Lett. B **355**, 318 (1995) [hep-ph/9506201].

[4] Z. Ligeti, M. E. Luke, A. V. Manohar and M. B. Wise, Phys. Rev. D **60**, 034019 (1999) [hep-ph/9903305].

[5] C. W. Bauer, Phys. Rev. D **57**, 5611 (1998) [Erratum-ibid. D **60**, 099907 (1999)] [hep-ph/9710513].

[6] D. Benson, I. I. Bigi and N. Uraltsev, Nucl. Phys. B **710**, 371 (2005) [hep-ph/0410080].

[7] A. L. Kagan and M. Neubert, Eur. Phys. J. C **7**, 5 (1999) [hep-ph/9805303].

[8] G. P. Korchemsky and G. Sterman, Phys. Lett. B **340**, 96 (1994) [hep-ph/9407344].

[9] R. Akhoury and I. Z. Rothstein, Phys. Rev. D **54**, 2349 (1996) [hep-ph/9512303].

[10] M. Neubert, Phys. Rev. D **49**, 4623 (1994) [hep-ph/9312311]; Phys. Rev. D **49**, 3392 (1994) [hep-ph/9311325].

[11] I. I. Y. Bigi, M. A. Shifman, N. G. Uraltsev and A. I. Vainshtein, Int. J. Mod. Phys. A **9**, 2467 (1994) [hep-ph/9312359].

[12] K. S. M. Lee and I. W. Stewart, Nucl. Phys. B **721**, 325 (2005) [hep-ph/0409045].

[13] S. W. Bosch, M. Neubert and G. Paz, JHEP **0411**, 073 (2004) [hep-ph/0409115].

[14] M. Beneke, F. Campanario, T. Mannel and B. D. Pecjak, JHEP **0506**, 071 (2005) [hep-ph/0411395].

[15] M. Neubert, Eur. Phys. J. C **40**, 165 (2005) [hep-ph/0408179].

[16] S. W. Bosch, B. O. Lange, M. Neubert and G. Paz, Nucl. Phys. B **699**, 335 (2004) [hep-ph/0402094].

[17] C. W. Bauer and A. V. Manohar, Phys. Rev. D **70**, 034024 (2004) [hep-ph/0312109].

[18] B. O. Lange and M. Neubert, Phys. Rev. Lett. **91**, 102001 (2003) [hep-ph/0303082].

[19] S. Chen *et al.* [CLEO Collaboration], Phys. Rev. Lett. **87**, 251807 (2001) [hep-ex/0108032].

[20] P. Koppenburg *et al.* [Belle Collaboration], Phys. Rev. Lett. **93**, 061803 (2004) [hep-ex/0403004];
K. Abe *et al.* [Belle Collaboration], hep-ex/0508005.

[21] B. Aubert *et al.* [BaBar Collaboration], hep-ex/0508004.

[22] G. P. Korchemsky and A. V. Radyushkin, Nucl. Phys. B **283**, 342 (1987); I. A. Korchemskaya and G. P. Korchemsky, Phys. Lett. B **287**, 169 (1992).

[23] M. E. Luke and A. V. Manohar, Phys. Lett. B **286**, 348 (1992) [hep-ph/9205228].

[24] A. F. Falk, M. Neubert and M. E. Luke, Nucl. Phys. B **388**, 363 (1992) [hep-ph/9204229].

[25] K. Melnikov and A. Mitov, Phys. Lett. B **620**, 69 (2005) [hep-ph/0505097].

[26] A. F. Falk and M. Neubert, Phys. Rev. D **47**, 2965 (1993) [hep-ph/9209268].

[27] T. Mannel, Phys. Rev. D **50**, 428 (1994) [hep-ph/9403249].

[28] M. Gremm and A. Kapustin, Phys. Rev. D **55**, 6924 (1997) [hep-ph/9603448].

[29] I. I. Y. Bigi, M. A. Shifman, N. G. Uraltsev and A. I. Vainshtein, Phys. Rev. D **52**, 196 (1995) [hep-ph/9405410].

[30] I. I. Y. Bigi, M. A. Shifman, N. G. Uraltsev and A. I. Vainshtein, Phys. Rev. D **50**, 2234 (1994) [hep-ph/9402360].

[31] M. Beneke and V. M. Braun, Nucl. Phys. B **426**, 301 (1994) [hep-ph/9402364].

[32] G. Martinelli, M. Neubert and C. T. Sachrajda, Nucl. Phys. B **461**, 238 (1996) [hep-ph/9504217].

[33] M. Neubert, Phys. Lett. B **393**, 110 (1997) [hep-ph/9610471].

[34] M. Neubert, Phys. Lett. B **612**, 13 (2005) [hep-ph/0412241].

[35] B. O. Lange, M. Neubert and G. Paz, hep-ph/0504071, to appear in Phys. Rev. D.

[36] D. Benson, I. I. Bigi, T. Mannel and N. Uraltsev, Nucl. Phys. B **665**, 367 (2003) [hep-ph/0302262].

[37] A. H. Hoang, Z. Ligeti and A. V. Manohar, Phys. Rev. D **59**, 074017 (1999) [hep-ph/9811239].

[38] M. Beneke, Phys. Lett. B **434**, 115 (1998) [hep-ph/9804241].

[39] P. Gambino and N. Uraltsev, Eur. Phys. J. C **34**, 181 (2004) [hep-ph/0401063].

[40] I. I. Y. Bigi, M. A. Shifman and N. Uraltsev, Ann. Rev. Nucl. Part. Sci. **47**, 591 (1997) [hep-ph/9703290].

[41] T. Mannel and M. Neubert, Phys. Rev. D **50**, 2037 (1994) [hep-ph/9402288].

[42] O. V. Tarasov, A. A. Vladimirov and A. Y. Zharkov, Phys. Lett. B **93**, 429 (1980).

[43] S. Moch, J. A. M. Vermaseren and A. Vogt, Nucl. Phys. B **688**, 101 (2004) [hep-ph/0403192].

[44] G. P. Korchemsky and G. Marchesini, Nucl. Phys. B **406**, 225 (1993) [hep-ph/9210281].

[45] E. Gardi, JHEP **0502**, 053 (2005) [hep-ph/0501257].

[46] X. Garcia i Tormo, M. Neubert and I. Scimemi, in preparation.